THESIS FOR THE DEGREE OF DOCTOR OF PHILOSOPHY

Studies of Glycosaminoglycan Interactions

Surface Immobilization Strategies and Biosensing Applications

NOOMI ALTGÄRDE

CHALMERS

Department of Applied Physics

CHALMERS UNIVERSITY OF TECHNOLOGY

Göteborg, Sweden 2014

Studies of glycosaminoglycan interactions
- surface immobilization strategies and biosensing applications
NOOMI ALTGÄRDE

ISBN 978-91-7597-128-5

Doktorsavhandlingar vid Chalmers tekniska högskola
Ny serie nr 3809
ISSN 0346-718X

Division of Biological Physics
Department of Applied Physics
Chalmers University of Technology
SE-412 96 Göteborg
Sweden
Telephone + 46 (0)31-772 1000
e-mail: noomi.altgarde@chalmers.se

Cover picture:
Glycosaminoglycans in the extra cellular matrix and at the cell membrane serves many different functions. For full figure caption, see Figure 1.

Funding:
The research leading to these results has received funding from the European Union Seventh Framework Programme (FP7/2007– 2013) under Grant Agreement No. NMP4-SL2009-229292 (“Find & Bind”), and from the Swedish Research Council (VR) through the Linneaus program SUPRA.

Printed by Chalmers Reproservice
Gothenburg, Sweden 2014

Studies of glycosaminoglycan interactions
- surface immobilization strategies and biosensing applications

NOOMI ALTGÄRDE
Division of Biological Physics, Department of Applied Physics
Chalmers University of Technology

Abstract

Many important biological functions of glycosaminoglycans (GAGs) have been highlighted in research literature during recent years. GAGs often serve as function-bearing structural elements in the extracellular matrix (ECM), but are also constituents of the cell membrane. GAGs take part in various biological mechanisms, e.g. regulating tissue growth and maintenance, as well as in the development of different diseases. The varying chemical structure of GAGs promotes interesting properties, but also makes them challenging to study. Surface-based analytical techniques can provide detailed information about the many interactions that GAGs participate in. This requires immobilization of one of the interacting entities in a biofunctional manner to ensure reliability of the subsequent interaction studies.

In this thesis, different methods for immobilizing GAGs to surfaces were investigated with the aim of studying GAG-related interactions. The GAGs chondroitin sulfate (CS) and hyaluronan (HA), as well as synthetically sulfated derivatives were primarily used. Immobilization was made to supported lipid bilayers on silica and self-assembled monolayers on gold, either using native GAGs or variants functionalized with e.g. biotin. The formation of GAG-based layer-by-layer assemblies was also studied. Immobilization and subsequent interactions were followed in real-time using quartz crystal microbalance with dissipation monitoring (QCM-D) and surface plasmon resonance (SPR)-based sensing. Interaction studies with various biological entities were made. The interactions were highly dependent on the orientation of the GAGs on the surface, and pros and cons associated with side-on versus end-on immobilization are discussed in the thesis. The immobilization strategy, especially if functional groups were introduced on the GAG, also influenced how the GAG was recognized by an interacting protein. Further, sulfated GAGs are known to serve as attachment factors for certain viruses, and binding studies of a herpes simplex virus glycoprotein to immobilized GAGs revealed interesting characteristics of certain regions on the protein. Also the initial effect of chondrocytes on immobilized HA was studied using combined surface sensing and light microscopy. The results presented here emphasize important aspects to consider when designing GAG-based interaction platforms, and exemplifies important biological studies that can be made by utilizing such platforms.

Keywords: glycosaminoglycans, surface immobilization, interaction studies, growth factor, virus glycoprotein, QCM-D, SPR

Gabriel. Be curious. Be wise. Be happy.

Appended Papers

Paper I

Immobilization of Chondroitin Sulfate to Lipid Membranes and its Interactions with ECM Proteins

Noomi Altgärde, Jana Becher, Stephanie Möller, Franz E. Weber, Matthias Schnabelrauch, Sofia Svedhem

Journal of Colloid and Interface Science 390 (2013) 258–266

I was responsible for designing and planning the experimental work. I performed all the experiments concerning GAG-immobilization and protein interactions. I wrote the main part of the manuscript.

Paper II

Probing the biofunctionality of biotinylated hyaluronan and chondroitin sulfate by hyaluronidase degradation and aggrecan interaction

Noomi Altgärde,[†] Erik Nilebäck,[†] Laura De Battice, Jana Becher, Stephanie Möller, Matthias Schnabelrauch, Sofia Svedhem

[†]*Authors contributed equally*

Acta Biomaterialia 9 (2013) 8158–8166

I was, together with E.N., responsible for designing and planning the experimental work. I performed the experiments concerning immobilization of GAGs for interaction studies using aggrecan, as well as additional physico-chemical characterization of the GAG layers. I wrote the main part of the manuscript.

Paper III

Mucin-like region of herpes simplex virus type 1 attachment protein gC modulates the virus-glycosaminoglycan interaction

Noomi Altgärde, Charlotta Eriksson, Edward Trybala, Stephanie Moeller, Matthias Schnabelrauch, Sofia Svedhem, Tomas Bergström, Marta Bally

In manuscript (2014)

I was, together with M.B., responsible for planning and performing the experimental work regarding the gC-GAG interaction studies. I wrote the main part of the manuscript.

Paper IV

Acoustic monitoring of changes in well-defined hyaluronan layers exposed to chondrocytes

Erik Nilebäck, Lars Enochson, Noomi Altgärde, Matthias Schnabelrauch, Anders Lindahl, Sofia Svedhem, Angelika Kunze

Analyst 139 (2014) 5350-5353

I participated in designing and performing the experiments, and proofreading of the manuscript.

Paper V

Tuning Cell Adhesion and Growth on Biomimetic Polyelectrolyte Multilayers by Variation of pH During Layer-by-Layer Assembly

Neha Aggarwal, Noomi Altgärde, Sofia Svedhem, Georgios Michanetzis, Yannis Missirlis, Thomas Groth

Macromolecular Bioscience 13 (2013) 1327–1338

I took part in the QCM-D measurements and especially in the interpretation of the data. I was involved in writing the manuscript, particularly concerning QCM-D.

Papers not included in the thesis

Effect of Molecular Composition of Heparin and Cellulose Sulfate on Multilayer Formation and Cell Response
Neha Aggarwal, Noomi Altgärde, Sofia Svedhem, Kai Zhang, Steffen Fischer, Thomas Groth
Langmuir 29 (2013) 13853-13864

Peptide-membrane interactions of arginine-tryptophan peptides probed using quartz crystal microbalance with dissipation monitoring
Hanna Rydberg, Angelika Kunze, Nils Carlsson, Noomi Altgärde, Sofia Svedhem, Bengt Nordén
European Biophysics Journal 43 (2014) 241-253

Study on multilayer structures prepared from heparin and semi-synthetic cellulose sulfates as polyanions and their influence on cellular response
Neha Aggarwal, Noomi Altgärde, Sofia Svedhem, Kai Zhang, Steffen Fischer, Thomas Groth
Colloids and Surfaces B: Biointerfaces 116 (2014) 93–103

Abbreviations

BMP-2: bone morphogenetic protein-2

CS: chondroitin sulfate

DS: dermatan sulfate

ECM: extracellular matrix

EDC: N-(3-Dimethylaminopropyl)-N′-ethylcarbodiimide hydrochloride

GAG: glycosaminoglycan

gC: glycoprotein

HA: hyaluronan, hyaluronic acid, hyaluronate

HS: heparan sulfate

HSV: herpes simplex virus

LbL: layer-by-layer

NHS: N-hydroxysuccinimide

SA: streptavidin

SAM: self-assembled monolayer

sHA: sulfated hyaluronan

SLB: supported lipid bilayer

SPR: surface plasmon resonance

QCM-D: quartz crystal microbalance with dissipation monitoring

Table of Contents

1 Introduction **1**
1.1 Aim 2

2 Structure of glycosaminoglycans **3**
2.1 The importance of sulfation 5
2.2 Synthetic modifications 5

3 Function and utilization of glycosaminoglycans **7**
3.1 Anticoagulants 8
3.2 Tissue maintenance 9
3.2.1 *In vivo* structural support 9
3.2.2 Involvement in cancer progression 9
3.2.3 Regulation of growth factor signaling 10
3.2.4 Components in cell scaffolds 10
3.3 Attachment factors for microbial pathogens 11

4 Designing glycosaminoglycan-presenting surfaces **13**
4.1 Inert backgrounds 13
4.1.1 Supported Lipid Bilayers 13
4.1.2 Self-Assembled Monolayers 15
4.2 Immobilizing biomolecules 15
4.2.1 Introducing functional groups 15
4.2.2 Covalent coupling 16
4.2.3 Biotin-avidin binding 17
4.2.4 Molecular adsorption and the layer-by-layer technique 18

5 Studying glycosaminoglycan interactions **19**
5.1 Specificity 19
5.2 Multivalency 20
5.3 Quantifying binding characteristics 20

6 Experimental techniques **23**
6.1 Quartz Crystal Microbalance with Dissipation Monitoring 23
6.1.1 Modeling of QCM-D data 24
6.2 Surface Plasmon Resonance 26
6.3 Fluorescence Recovery After Photobleaching 28
6.4 Isoelectric point analysis 28
6.5 Contact angle goniometry 29

7 Results **31**
7.1 Summary of appended papers 31
7.2 Glycosaminoglycan library 32
7.3 Strategies to immobilize glycosaminoglycans 33
7.3.1 Covalent immobilization to supported lipid bilayers (Paper I) 33
7.3.2 Immobilization via biotin-streptavidin on self-assembled monolayers (Paper II-IV) 36
7.3.3 Build-up of layer-by-layer structures (Paper V) 39
7.4 Biofunctionality of immobilized glycosaminoglycans 40

7.4.1 Influence of introduced functional groups (Paper I & II) 40
7.4.2 Side-on vs. end-on immobilization (Paper II, additional results) 43
7.5 Biological applications of surface immobilized glycosaminoglycans 46
7.5.1 Binding of herpes simplex virus glycoprotein C (Paper III) 46
7.5.2 Initial effect of chondrocytes (Paper IV) 49
7.5.3 Interactions with bone morphogenetic protein 2 (additional results) 51

8 Perspectives and outlook **53**

9 Acknowledgements **57**

1
Introduction

Medical discoveries are ever evolving. They shed light on the complex mechanisms that can keep a human alive for a hundred years, increase the understanding of how diseases begin and development, and lead to new strategies to replace or improve lost or impaired functions. Often, these advances rely on developments in scientific areas other than medical science, such as imaging, bioinformatics, material science and sensor science.

To understand important functions at the organism level, detailed understanding of molecular mechanisms is key. In general, biomolecular studies can be divided into three major areas; *genomics*, studying the genetic material, *proteomics* involving studies of the proteins encoded in the genes, and *glycomics,* focusing on carbohydrates. Human genes have four building blocks, or nucleobases. A combination of three nucleobases, codes for one out of 20 amino acids, which in turn build up proteins. Carbohydrates, e.g., glycosaminoglycans (GAGs) that are the focus for this thesis, are not synthesized based on genetic templates, but consist of disaccharides built up from enzymatic reactions. The possible combinations of the different disaccharides are vast, making them highly diverse in both structure (Chapter 2) and function (Chapter 3).[1,2]

The function of a certain molecule for an organism becomes evident when the molecule is missing or when its level is altered, e.g., due to a disease. The basis of this function lies in the existence of numerous interaction patterns between the molecule and other entities in the body. Controlled studies of these interactions can give a more detailed understanding of the complex mechanisms in our body. Due to their obvious importance, genomics and proteomics have for long been the primary focus when studying biomolecular interactions, and GAGs have mainly been prescribed to have structural properties in the tissue. However, likely owing to their strategic *in vivo* location, GAG-related interaction are expected to be involved in many vital mechanisms in the human body (Chapter 3).[2,3]

Hitherto, interactions between GAGs and other biomolecules have been mostly studied using e.g., equilibrium dialysis, nuclear magnetic resonance (NMR), and isothermal titration calorimetry,[3] studies through which invaluable insights about the interactions that GAGs take part in have been gained. All of these are examples of *solution-based* techniques, where the interacting partners can move freely in a solution. *In vivo*, GAGs are mostly found attached to a protein core and/or to the cell membrane and in that sense not moving freely. Hence, it could be beneficial to study

GAG-related interactions having the GAG immobilized to a surface, which also allows the use of *surface-based* techniques (Chapter 6). Apart from mimicking the *in vivo* environment for a particular system, there are other general benefits with using a surface-based approach when studying biomolecular interactions. Perhaps most notably, the connection of surface-based techniques with different transducer elements based on e.g., mechanical, optical, or electrical phenomena, allows for various types of information to be gained, often in real-time. The sample consumption is often lower and regeneration of the surface can allow for analysis of multiple samples on the same surface. Also, surface-based techniques allow for the development of biosensors for fast diagnostic applications.[4,5]

Although surface-based analytical techniques can have many benefits, the requirement of immobilization can sometimes pose problems as it might disturb the natural functions of the immobilized biomolecule, or in other ways affect the studied interactions. Hence, a suitable surface and immobilization strategy has to be used to ensure that the generated information has biological significance (Chapter 4). Various methods can be used to reduce non-specific binding to the background. Supported lipid bilayers (SLBs) and self-assembled monolayers (SAMs) are examples of such surface modifications, which can be further functionalized to allow for immobilization of biomolecules via various chemistries.

Apart from a better understanding of biological processes, the insights gained from studying GAG-related interactions can contribute to medical discoveries with applications both *in vivo*, e.g., as new drugs, and *in vitro*, e.g., as cell culture surfaces and tissue scaffolds, with the possibility of improving the quality of life.

1.1 Aim

The aim of this thesis project has been to study GAG-related interactions using surface-based analytical techniques. It can be divided into two parts: i) evaluating different strategies for surface immobilization of GAGs compatible with common transducer substrates such as gold and silica. (**Paper I, II, V**), ii) utilizing the established surface platforms to study biologically relevant interactions with proteins and cells by monitoring optical and viscoelastic properties at the transducer interface (**Paper III, IV**).

2
Structure of glycosaminoglycans

The molecular structure of GAGs in vivo, as well as synthetic modifications that can be made to GAGs in vitro, are discussion in this chapter.

Glycosaminoglycans (GAGs) are long, unbranched polysaccharide chains consisting of repeated disaccharide units. One unit consists of two monosaccharides, one uronic sugar, containing a carboxyl group (with the exception of keratin sulfate) and one amino sugar, linked together by a glycosidic bond. The GAG chain has a structural direction by having a *reducing* and a *non-reducing* end (**Table 1**).

All GAGs except hyaluronan (HA) are found attached to a protein core, forming a *proteoglycan*. Proteoglycans are synthesized by most vertebrate cells and extend from the cell membrane or are secreted into the extracellular matrix (ECM).[1] The attachment of the GAG to the core protein begins in the endoplasmic reticulum and continues through the Golgi apparatus.[6] The GAG grows via its non-reducing end and is attached via the reducing end to the proteoglycan.[7] GAGs are also sulfated by sulfotransferases, creating a highly varying structure. The sulfation varies both in extent and placements on the saccharide, even within a certain GAG (section 2.1).[6,8] There are regions on the GAG chain displaying higher or lower (or no) sulfation, particularly prominent in heparan sulfate (HS). Other factors increasing the structural diversity of GAGs are the type of glycosidic bond, isomeric forms, and molecular weight.[2]

The GAG HA is neither sulfated, nor connected to a protein core. In contrast to GAGs that are part of a proteoglycan, HA grows from its reducing end. It is synthesized by the membrane-associated enzyme *hyaluronan synthase* and transported into the ECM as its being produced. When synthesized, it can either stay connected to the membrane via association with the synthase, or be released into the ECM.[9]

Interactions with enzymes, e.g., heparinases, chondroitinases, and hyaluronidase, depolymerize GAGs, regulating the amount of GAGs in the tissue.[2,10]

Table 1: Molecular structure and related specifics of glycosaminoglycans. [3,11-13]

	General structure	Specifics
Hyaluronan	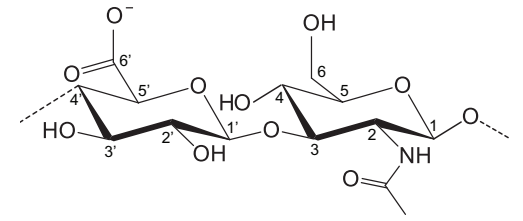 non-reducing end reducing end	Molecular weight: 10 -1000 kDa Not part of proteoglycans alternating β(1-4) and β(1-3) linkage
Chondroitin sulfate	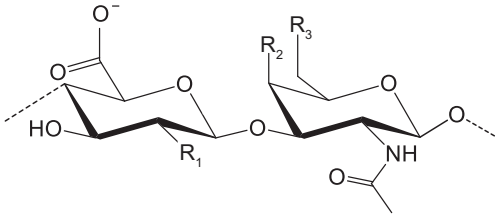	Molecular weight: 5 -50 kDa alternating β(1-4) and β(1-3) linkage **R_1** / **R_2** / **R_3** OH / OSO_3^- / OH — **CS-A** OH / OH / OSO_3^- — **CS-C** OSO_3^- / OH / OSO_3^- — **CS-D** OH / OSO_3^- / OSO_3^- — **CS-E**
Dermatan sulfate	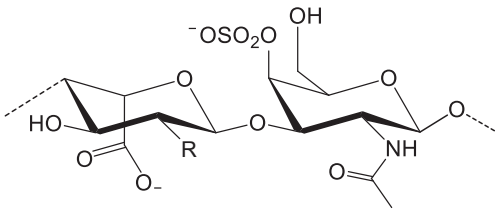	Molecular weight: 5 -50 kDa alternating β(1-4) and β(1-3) linkage **R** = OH, OSO_3^-
Keratan sulfate	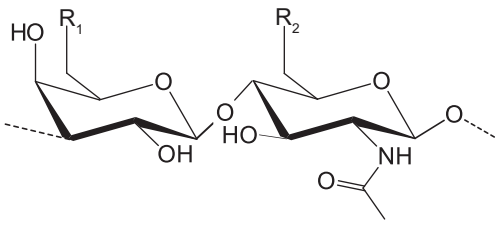	Molecular weight: 5 -50 kDa alternating β(1-4) and β(1-3) linkage **R_1** / **R_2** OH / OH OH / OSO_3^- OSO_3^- / OSO_3^-
Heparan sulfate/ Heparin	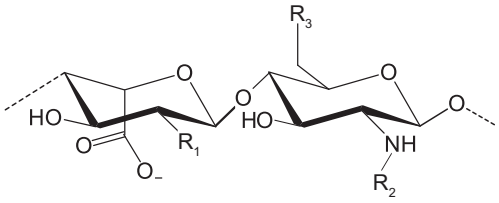	Molecular weight: 5-50kDa/ 1 -30 kDa α(1-4) linkage **R_1** / **R_2** / **R_3** OH / $COCH_3$ / OH — 50% of **HS*** OH / SO_3^- / OH OSO_3^- / SO_3^- / OH OH / SO_3^- / OSO_3^- OSO_3^- / SO_3^- / OSO_3^- — 80% of **heparin** * carboxyl group directed upwards

2.1 The importance of sulfation

GAG-related interactions are controlled to a large extent by the sulfation pattern of the GAG, e.g. evident as mutations resulting in the lack of sulfation cause severe developmental disorders.[14] The different sulfation patterns seen in GAGs have been shown to be specific for certain tissues, developmental stages and disease conditions.[1,15-18] HS, CS and DS all show a great diversity in their sulfation patterns, which is likely the reason why they have such multitude of functions. Considering the possible sulfation patterns listed in **Table 1**, HS can display 48 unique disaccharide blocks. This can be compared to DNA being built up by 4 unique nucleic acids, and proteins consisting of combinations of 20 different amino acids.[2] Sulfation is made during proteoglycan synthesis but sulfation of the C6 position can also be post-synthetically removed by the enzymes Sulf1 and Sulf2, which either inhibits or activates certain functions.[14] This plays a role in e.g. the binding of growth factors by HS (section 3.2.1),[14,19] and is a good example of how sulfation can fine-tune the function of GAGs.

2.2 Synthetic modifications

The structural diversity seen in GAGs makes them intriguing, but also challenging to study. GAGs isolated from animal and bacterial sources show great variability between batches, which sometimes results in difficulties when reproducing scientific findings. One approach to overcome such issues is to modify simpler GAGs or other polysaccharides to create GAG-derivatives or analogues. For example, *cellulose* that can be found in the cell wall of green plants consists of repeated units of the monosaccharide *glucose*. *Chitin* consists of N-glycosamine and N-acetyl-glucosamine units and can be extracted from e.g., crustaceans or fungi.[20,21] These polysaccharides can be modified by e.g., acetylation[22] and deacetylation,[20] carboxymethylation,[23] and sulfation[24-26] in order to function as GAG-analogues or to enhance some GAG-related properties, e.g., loading of growth factors[27]. Enzymatic changes can also be applied to native GAGs; in thesis work, HA was used as a starting material in producing sulfated GAGs by reaction with a SO_3-DMF (dimethylformamide) complex. The same strategy was also used to produce over-sulfated version of CS.[28,29]

However, when using animal sources for the extraction of GAGs, there is a risk of contamination. For example, immunogenic proteins or infectious entities like viruses that are associated with the GAG could be extracted as well. Also, the difference in availability of different GAGs, albeit their similar molecular structure, has led to incidents of willful contamination. During the Chinese heparin crisis in 2008, natural heparin for the use as an anticoagulant drug, was partially replaced by synthetically over-sulfated CS, resulting in numerous deceased patients.[30] The alternative to isolation from natural sources and chemical modification is to synthesize GAGs *de novo*. The structural complexity of GAGs and the need for protection and de-protection of multiple orthogonal chemical groups make conventional methods

suitable for the build-up of penta- and hexasaccharides only.[31,32] Another possible strategy to synthesize GAGs is by the use of enzymatic reactions.[31]

3
Function and utilization of glycosaminoglycans

Even when the significance and/or the mechanisms of a certain GAG-related function is difficult to establish in vivo, GAGs can serve important functions in vitro or when administered as a drug. In this chapter, some examples of the various functions that GAGs can serve in vivo and in vitro are presented.

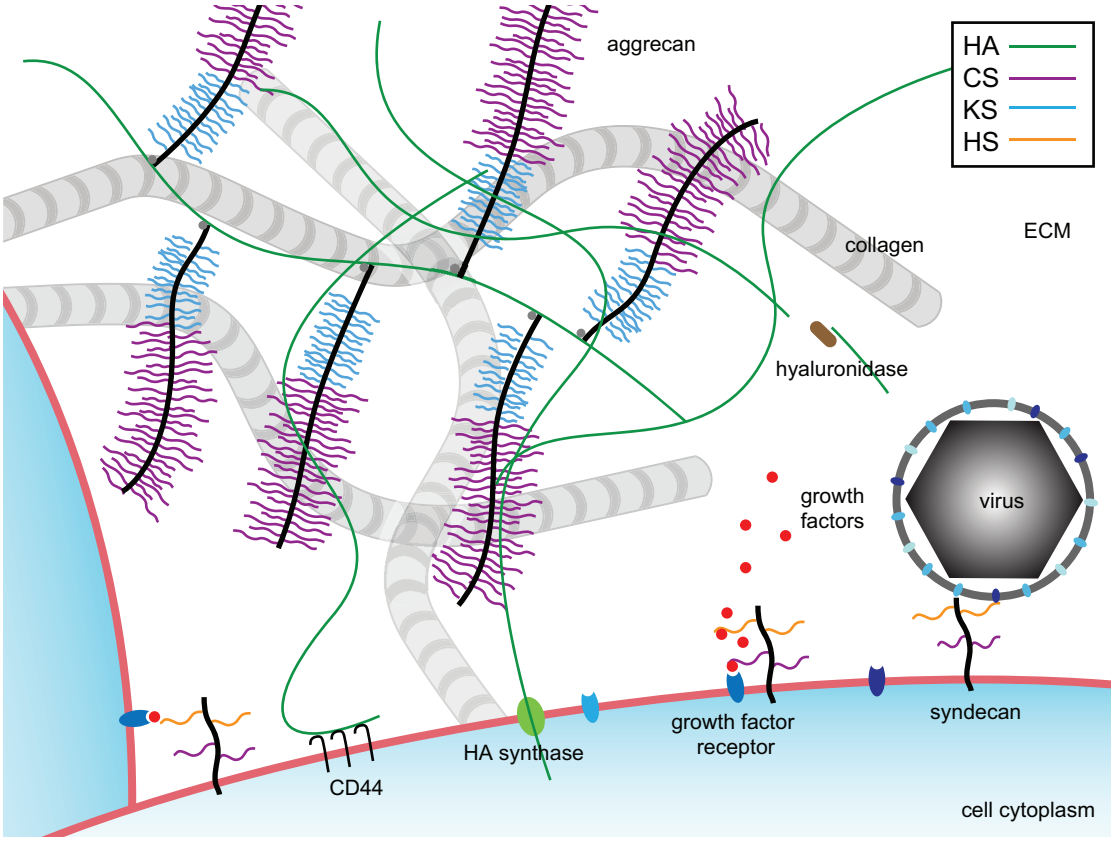

Figure 1. Examples of the various functions of GAGs in the extracellular matrix (ECM) and at the cell membrane. Hyaluronan (HA) extends from the surface of many cells, either via its synthase or via the receptor CD44, forming a glycocalyx. HA can also be found free in the ECM where it, in e.g. cartilage, forms larger supramolecular structures together with the proteoglycan aggrecan, carrying numerous keratin sulfate (KS) and chondroitin sulfate (CS) chains. Aggrecan also interacts with collagen fibrils. Chondroitin sulfate (CS) and heparan sulfate (HS) at the cell membrane serve as attachment factors for e.g. viruses and growth factors. Enzymes in the ECM, e.g. hyaluronidase can degrade GAGs. (Note that the figure is not a representative of a certain tissue, but exemplifies different GAG functions.)

3.1 Anticoagulants

Blood coagulation involves multiple molecular interactions that finally lead to the formation of a blood clot (*thrombus),* consisting of fibrin and platelets (*thrombocytes*). This cascade of interactions is regulated by many different proteins that either activate or inhibit coagulation (**Figure 2**). Precise control is crucial as both an inactive and an overactive coagulation can be life threatening.[33] In the early 20th century, the GAG heparin was found to have anticoagulant properties, and the mechanism was later confirmed to be through potentiation of the coagulation inhibiting enzymes *antithrombin III* and *heparin cofactor II* (**Figure 2**).[34] The first heparin drug was commercialized in the 1940s but since the action of heparin was ascribed to a specific pentasaccharide sequence,[35] it is today prescribed as depolymerized heparin (Fragmin®) or as a synthetic derivative of this pentasaccharide (Arixtra®).[36] DS, and to some extent CS-E (**Table 1**) has been shown to have similar abilities as heparin to activate heparin cofactor II.[37,38]

HA has no known heparin-like function on the coagulation cascade, likely due to the lack of sulfate groups.[39] However, HA-based surface coatings have been shown to have antifouling properties by limiting the adsorption of plasma protein and subsequent adhesion of platelets, thereby inhibiting the initiation of blood coagulation.[40-42] This is likely due to the masking of an otherwise thrombotic surface, and to the hydrophilic character of HA. This could potentially be utilized for coating of coronary stents, as stent-induced thrombosis is a major clinical problem.[43]

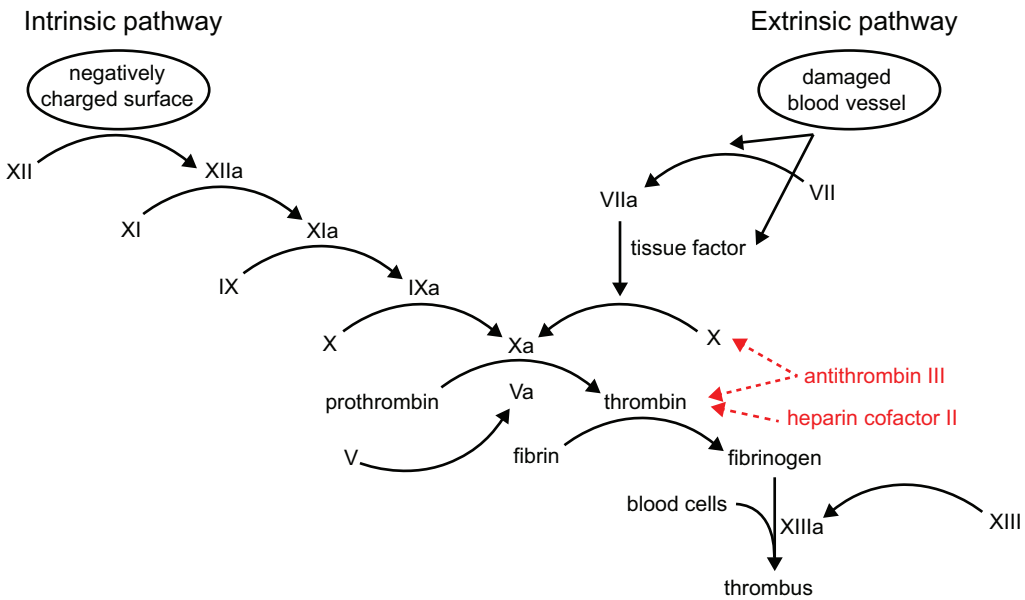

Figure 2. Simplified schematic of the intrinsic and extrinsic pathways of the coagulation cascade. Heparin/HS inhibits coagulation by enhancing the activity of the inhibitors antithrombin III and heparin cofactor II.

3.2 Tissue maintenance

3.2.1 *In vivo* structural support

GAGs are major constituents of the ECM where it can interact with other GAGs and ECM proteins, forming extensive supramolecular assemblies around the cells. As an example, the proteoglycan aggrecan with multiple CS and KS chains, binds via the N-terminal of the core protein to HA chains, together with a link protein (**Figure 1**).[44] This complex can in turn associate with the cell membrane via the HA-receptor CD44, further stabilizing the ECM.[45] The stability of HA-aggrecan assemblies is pH dependent and is therefore thought to be involved in tissue responses to inflammation. This is also supported by the fact that HA binds an inflammation-response protein, TSG-6.[46] Aggrecan can also build up supramolecular assemblies with collagen, the most abundant protein in the ECM.[47] Both the protein core and the GAG chain on aggrecan participate in this interaction, which is likely dominated by electrostatics as there is a strong dependence on ionic strength and pH.[48]

As the long and hydrophilic GAG chains also extend from the cell surfaces, they serve as cushions and lubricants around cells.[49,50] This feature is especially important around chondrocytes in cartilage[51] but can also function as a protective barrier around other cells, e.g. ovary cells.[52]

3.2.2 Involvement in cancer progression

Patients suffering from cancer often have an increased risk for thrombosis, and for a long time, a common treatment has therefore been with anticoagulants such as heparin (section 3.1). As a positive side effect of this treatment, it has been shown in numerous studies that heparin also had an effect on the progression of the cancer itself. Multiple mechanisms describing this effect of heparin have been suggested; e.g., inhibition of metastasis by inhibiting cancer cell-induced thrombosis and an effect on angiogenesis and proliferation through the involvement in growth factor signaling (section 3.2.2). Considering the multiple effects of heparin and other GAGs, it is not surprising that studies investigating their effect in cancer suggest both inhibitory and stimulatory effects on cancer progression. Most studies involve full-length heparin, and low-molecular weight heparin might provide the needed response-control.[17,53]

3.2.3 Regulation of growth factor signaling

The presence of GAGs in the ECM as well as at the cell membrane is ideal for the involvement in extracellular and cell signaling events. *Growth factors* are small substances that convey signals between cells by binding to cell surface receptors, and thereby regulating cell proliferation and differentiation. *Fibroblast growth factors* (FGFs) are known to interact with HS-chains on proteoglycans in the cell membrane, which is likely a requirement for FGFs to bind to their receptor.[14,54] *Bone morphogenetic protein 2* (BMP-2) is a member of the transforming growth factor β (TGF-β) superfamily that has been shown to induce bone formation *in vivo* and to promote cell differentiation towards the osteoblast linage *in vitro*.[55,56] It is therefore a promising candidate to be used in research and in clinic to ameliorate bone formation. However, *in vivo* administration of growth factors suffers from short lifetimes due to rapid degradation in the ECM. Therefor different combinations of growth factors with a stabilizing agent are sought. Combining growth factors and GAGs has been shown to increase the lifetime of growth factors[14,54], and to e.g. improve the effect of BMP-2 *in vivo* [57].

3.2.4 Components in cell scaffolds

The structural properties of GAGs make them suitable to use in the engineering of scaffold used for directed cell growth *in vitro* and *in vivo*.[58] CS and collagen is frequently combined to form scaffolds, and has e.g. been shown to support the adhesion of stem cell and differentiation towards the osteoblast lineage.[59] Functionalized and/or cross-linked HA is also often used as scaffold materials in both research and in clinic. For example, the commercially available HYAFF® consists of HA were the carboxyl groups are esterified by the addition of hydroxyl groups (e.g. benzyl alcohol), which gives HA increased hydrophobicity, increased attachment to cells, and slower degradation.[60] For example, cartilage defects are treated by the use of a HYAFF® scaffold seeded with patient-own chondrocytes.[61] Also less invasive techniques are being developed for bone and cartilage application, e.g. by injecting functionalized HA and a polymer showing a complementary chemistry, e.g. thiol-acrylate.[62] Surface coatings are often used to improve the ingrowth of biomaterials into tissues *in vivo*. Adsorbing multiple layers of polyelectrolytes, e.g. GAGs, is a straightforward way to coat biomaterials of various sizes and geometries (section 4.2.4), and can be used to tune the response from surrounding cells.[63]

Due to the positive effects of combining GAGs with growth factors, discussed in section 3.2.2, the addition of growth factors to the scaffolds mentioned above can be beneficial in many tissue-engineering applications. For example, multilayered polyelectrolyte structures have been loaded with BMP-2[64,65] and FGF-2[66] and used for cell growth *in vitro*. A significant release may not be necessary for activity of the growth factor, e.g. BMP-2 loaded in a HA scaffold was proposed to work in concert with the GAG while still in the structure.[67] Also the HA-based scaffolds mentioned above are often combined with growth factors.[61,68]

3.3 Attachment factors for microbial pathogens

Infectious diseases occur when pathogenic microorganisms spread in the body. The ability for a microbe to localize in the body is often mediated by interactions with, and often by entry into cells. Viruses are small (~10^2 nm) pathogens that enter cells in order to hijack the replication machinery, as they lack one of their own. The infection of a cell by a virus can be divided into six major steps that are common for all virus types: *attachment, penetration, uncoating, replication, assembly* and *release.* When the new virus particles, *virions*, are released, they can infect other cells nearby. Many viruses, e.g. herpes simplex virus (HSV),[69,70] respiratory syncytial virus (RSV),[69,71] Ebola virus,[72] and HIV,[73] utilize cell surface GAGs as attachments factors (**Figure 3**). The herpes simplex virus type 1 (HSV-1) has been extensively studied in this aspect, where glycoprotein C in the viral envelope has been identified as binding to cell surface HS and CS.[74,75] The GAG-binding region on the glycoproteins is thought to consist of clusters of positively charged amino acid residues that can bind to sulfated GAGs.[75-78]

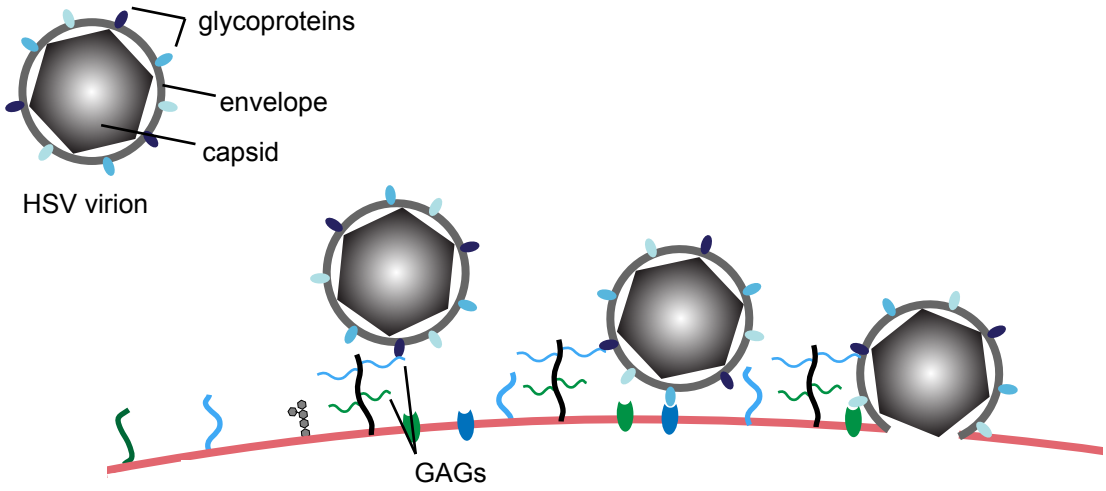

Figure 3. Simplified illustration of a herpes simplex virus entering a host cell via attachment and membrane fusion between the viral lipid envelope and the host cell membrane.

Also certain bacteria (Helicobacter pylori, Bordetella pertussis, Chlamydia trachomatis) and other parasites (Plasmodium and Leishmania) have been shown to present GAG-binding proteins on their surfaces that are likely to be important in how they interact with host organisms.[79]

The fact that GAGs act as attachment factors for different microbes opens up for the possibility of using GAGs as antimicrobial agents, where binding could potentially prevent attachment of the microbe and further effects on the host cell. This approach could in some case be better than the reverse, i.e. to block receptors on the host cell, since these receptors might also serve other important purposes for the cell.[80] There are many *in vitro* studies suggesting an inhibitory effect on different microbes by the

addition of GAGs: e.g., HS/heparin can inhibit the attachment of the herpes simplex virus, respiratory syncytial virus and Japanese encephalitis virus to cells.[69,81,82] HS has also been shown to inhibit attachment of HIV to cells by binding to the enveloped viral glycoprotein gp120.[83] *Plasmodium falciparum*, the parasite causing the most dangerous type of malaria, has a very complex infectious cycle involving both mosquitos and humans. In one step, human erythrocytes infected with the parasite binds to the surface of endothelial cells, a step that can be inhibited by the addition of CS-A.[84]

The antimicrobial activity of GAGs usually increases with the molecular weight, but the large size and high charge of the GAGs can limit their ability to penetrate tissue.[85] To ensure better reproducibility and to limit side-effects, short, synthetic versions of GAGs are attractive to use.[86,87] A limiting aspect of using GAGs as antimicrobial agent is that a continuous administration is likely needed, as GAGs are known to inhibit binding of, but not to destroy, microbes.

One should note that there are many other polysaccharides apart from GAGs (and therefore not discussed in this thesis) present on microbes that could potentially be used in the discovery of new antimicrobial drugs.[36]

4

Designing glycosaminoglycan-presenting surfaces

In this chapter, general aspects of biomolecular immobilization are discussed and exemplified by strategies and techniques of relevance for this thesis project, i.e. with a focus on biosensing. Examples from the literature where the different strategies have been used for immobilizing GAGs are also given.

Immobilization of biomolecules to surfaces is a mean to control biomaterial properties, and also opens up for interaction studies using surface-based analytical techniques. Often, these techniques offer advantages over solution-based techniques, such as reduction of sample volumes. However, immobilization of one of the interaction partners is a requirement, which can be a limiting as well as a compromising factor. Care has to be taken to ensure that the immobilized molecule is still active, and to minimize non-specific interactions with the surface background.

In the literature, there are many examples of immobilization of short glycans for the purpose of interactions studies. Especially *glycan arrays*, where different mono-, di-, and short oligosaccharides are immobilized to a surface, have been extensively used to probe interactions in a high throughput manner, and to study the influence of defined saccharide structures.[88,89] Various immobilization strategies have been used for this, usually via the reducing end of the short saccharides.[90] Immobilization of full-length GAGs is generally less common. However, the literature that is referred to in this chapter exemplifies immobilization of oligomeric and polymeric GAG derivatives. In this thesis, the *ligand* refers to the immobilized molecule, and the *analyte* to the molecule added in solution.

4.1 Inert backgrounds

In order to obtain a desired function when immobilizing a biomolecule to a surface, it is often important to ensure an inert background. Two examples of such background surfaces are supported lipid bilayers (phospholipid membranes) and oligo(ethylene glycol)-modified surfaces.

4.1.1 Supported Lipid Bilayers

A supported lipid bilayer (SLB) is a simple model mimicking the lipid membrane component of a cell membrane, relying on the self-assembly of lipid molecules.[91] Lipids have a hydrophilic head and a hydrophobic tail (**Figure 4a**), allowing them to form ordered structures when dissolved in certain solvents. In water, lipids can

arrange into *vesicles*, i.e., spherical bilayer structures with the heads directed to the water inside and outside the vesicle and the tails directed into the bilayer (**Figure 4b**).

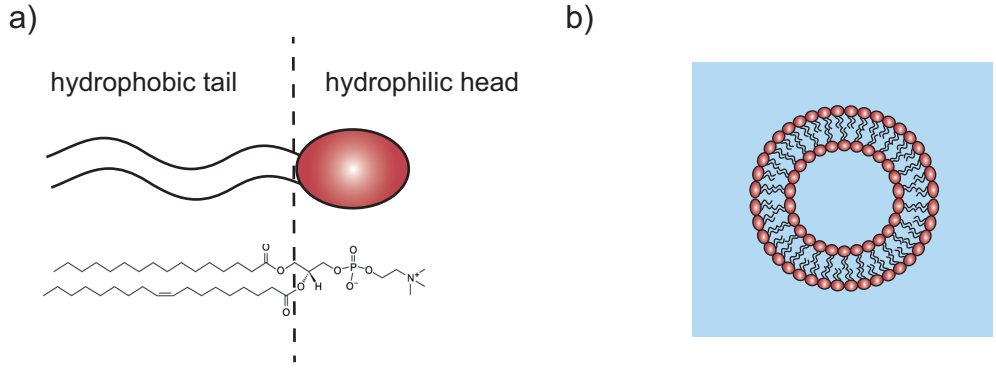

Figure 4. a) Schematic and chemical structure of a lipid, here 1-palmitoyl-2-oleoyl-*sn*-glycero-3-phosphocholine (POPC). b) Lipids self-assemble into vesicles in a water solution.

Commonly used methods for the formation of SLBs on solid surfaces include vesicle rupture (**Figure 5**)[92] and also the Langmuir-Blodgett technique[93]. Vesicle rupture during physiological conditions is commonly seen on hydrophilic surfaces like silica[94] and mica[95] but not on gold[94] and titania[94-96]. These limitations can be overcome by optimizing the conditions during the bilayer formation, after which the physiological conditions are restored. For example, pH,[96] ionic strength,[97] or the presence of divalent cations[92] can be tuned to enhance the interaction between the vesicles and the surface. Lipids in a self-assembled structure are often mobile, and cell membranes and lipid vesicles therefore normally show a certain degree of fluidity. This characteristic can, in the absence of a strong interaction between the lipid head group and the surface, be kept also in a SLB (see section 6.3).[98] SLBs combined with surface-based techniques are extensively used as model systems to study processes taking place at or near a cell membrane. Due to the lateral mobility of the lipids, and the fact that certain SLBs are good in minimizing non-specific interactions, they are often modified to extend their usability in interaction studies.[99-101]

In **Paper I**, functionalized SLBs were used for covalent immobilization of CS via two different strategies.

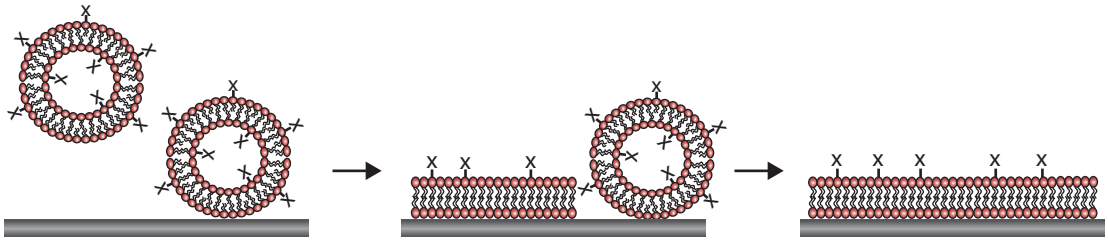

Figure 5. Formation of a SLB on a silica surface. Vesicles adsorb and, when a critical coverage of is reached, rupture. Lipids functionalized with various chemical groups (x) can be incorporated in the vesicles and be a target for immobilization.

4.1.2 Self-Assembled Monolayers

A self-assembled monolayer (SAM) refers to a single layer of molecules on a solid support formed from a spontaneous assembly.[102] With the objective of forming close-packed, oriented monolayer structures, alkanethiols adsorbing on a gold surface have been extensively studied (**Figure 6**). The semi-covalent bond between gold and sulfur in the thiol creates a strong link to the surface, and the non-thiolated end of the alkane chain can be functionalized with a chemically active group in order to bind other biomolecules.[103] It is preferred that binding only occurs to these functional groups, and the use of poly(ethylene) glycol (PEG) or oligo(ethylene) glycol (OEG) chains as a part of the alkanes have been found to minimize unspecific binding of proteins,[104] also in combination with various functional groups e.g., carboxyl,[104] and biotin groups[105].

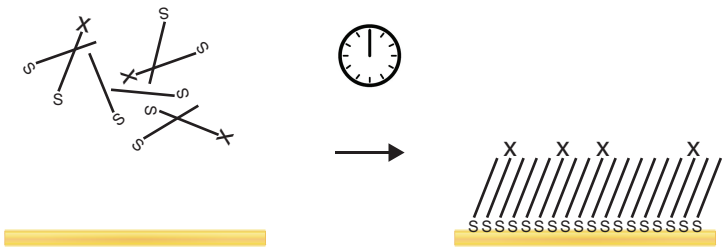

Figure 6. Formation of a self-assembled monolayer. A gold surface is incubated in a solution containing thiol molecules for >12h. The high degree of orientation of the thiols allows for immobilization to a functional group (x) on the other end of the thiol molecule.

SAMs functionalized with biotin was used in **Paper II, III & IV** for immobilization of various biotinylated GAG-derivatives.

4.2 Immobilizing biomolecules

In order to obtain a stable surface modification, it is important to form a strong bond between the biomolecule of choice and the model surface. The orientation of the immobilized molecules, as well as the density of immobilized molecules on the surface is also important.

4.2.1 Introducing functional groups

Biomolecules commonly contain various functional groups that can react with a suitable chemical group on a surface. Carboxyl, hydroxyl, and amine groups are typical examples of such functional groups. To extend the number of possible immobilization strategies, the biomolecule to be immobilized can be functionalized with foreign chemical groups. As GAGs are long, linear molecules, immobilization can either be made to multiple groups along the chain, resulting in a *side-on* immobilization, or to a single group at the end of the chain, resulting in an *end-on* immobilization of the GAG. This is independent on whether the GAG is functionalized or not (**Figure 7**).

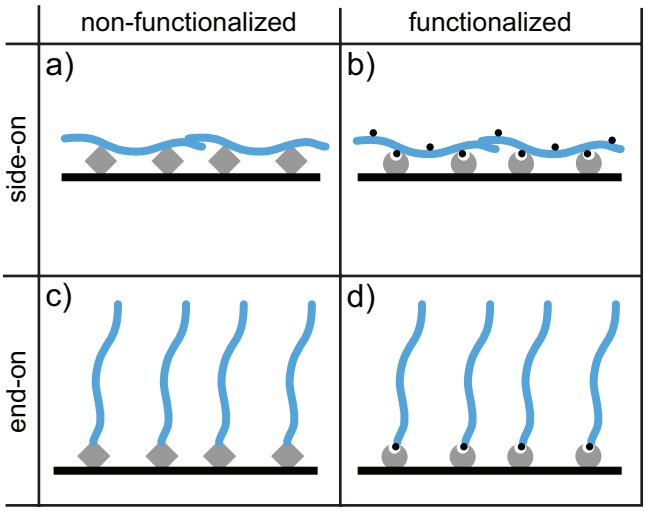

Figure 7. Surface immobilization of GAGs can be made using either non-functionalized (a, c) or functionalized GAGs (b, d). Immobilization via multiple groups along the GAG chain results in a side-on configuration (a, b). If immobilization is made via a single functionality at the end of the GAG chain, an end-on configuration is obtained (a, b).

4.2.2 Covalent coupling

Covalent coupling provides a strong bond between the biomolecule and the surface. When used in biosensing, it often enables regeneration of the sensor surface, which saves both time and material. The reaction between carboxyl groups and primary amines, forming *amide bonds*, is commonly employed for covalent immobilization of biomolecules.[106] In the *in vivo* synthesis of proteins, the amide bond formation between the amino acids is a reaction catalyzed by the action of many enzymes and other molecules. *In vitro*, the use of coupling reagents is necessary for the reaction to take place. For example, the carboxyl group can be converted to a so called *active ester* by the use of N-(3-dimethylaminopropyl)-N′-ethylcarbodiimide hydrochloride (EDC). However, the EDC-ester is easily hydrolyzed in water, which is why the addition of N-hydroxysuccinimide (NHS) is common. NHS creates a more stable ester that efficiently reacts with the amine group (or other nucleophilic groups) of the ligand in water and at physiological pH (**Figure 8**).[106,107] As a last step, ethanolamine is usually used to deactivate remaining carboxyl groups.

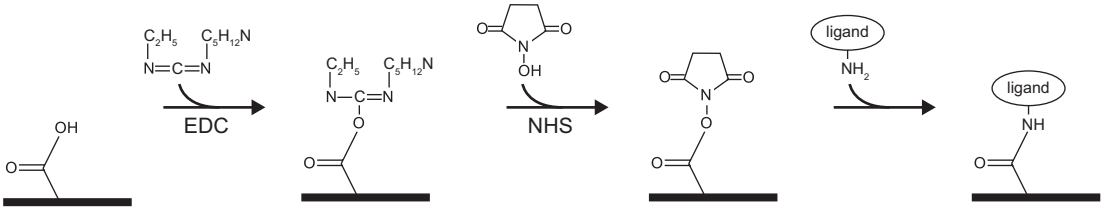

Figure 8. A surface-bound carboxyl group reacts with a primary amine on a ligand and forms an amide bond. EDC and NHS are used as coupling reagents.

The above mentioned strategy has e.g. been used to immobilize GAGs to chitosan-coated surfaces by coupling the carboxyl groups of the GAGs to primary amines in chitosan.[108] The surfaces were designed to support mesenchymal stem cell growth. Other covalent strategies that have been used for the immobilization of GAGs include e.g., direct coupling of GAGs via the reducing end to a hydrazide-[109] or primary amine-[110] presenting surface. There are also examples of functionalized GAGs being used. For example, carboxyl groups along the chain of high molecular weight GAGs, and the reducing end of a low molecular weight GAGs, were functionalized with hydrazide groups to allow for immobilization to polydopamine-coated microtiter plates.[111] The carboxyl groups of various GAGs have been functionalized with thiols, for the coupling to vinyl-terminated SAMs (section 4.1.2).[112] Photo-coupling of HA to silicon rubber by the use of 4-benzoylbenzoic acid, has also been reported.[113]

In this work, a covalent approach was used in **Paper I**, where CS was immobilized to two different SLBs.

4.2.3 Biotin-avidin binding

The strong interaction ($K_D \approx 10^{-15}$ M) between biotin and avidin has been used to immobilize biomolecules to surfaces for decades.[114] Bacterially derived streptavidin (SA) can be used instead of avidin, also exhibiting a strong binding to biotin ($K_D \approx 10^{-13}$ M) (**Figure 9**). SA is non-glycosylated and has a pI closer to neutral pH (pI ≈ 5-6) and therefore shows lower non-specific interactions.[115] Also neutravidin (pI = 6.3), a de-glycosylated variant of avidin, is sometimes used.[116] All of the three variants have four binding sites for biotin. The biotin-avidin interaction is compatible with a range of conditions in terms of pH and temperature and has been used for a number of different systems, such as studies of DNA hybridization,[100] and interaction studies involving proteins[117] and polymers[118] to mention some.

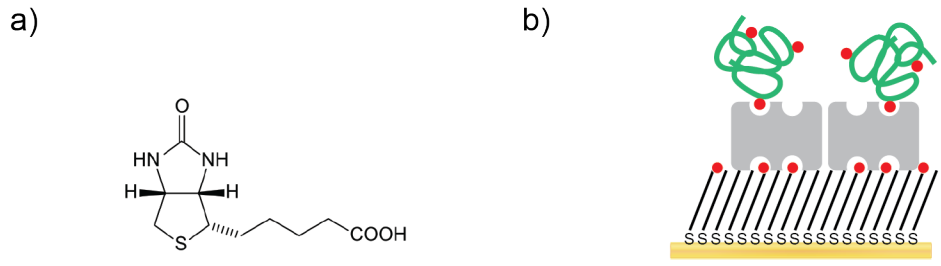

Figure 9. a) The chemical structure of biotin. b) Schematic illustration of a biomolecule immobilized using the interaction between biotin (red) and streptavidin (grey) on a self-assembled monolayer.

For the immobilization of GAGs using this strategy, commercial sensor chips used for SPR-based sensing, consisting of a dextran matrix functionalized with SA, are often used. To enable immobilization, the amine groups along GAG chains are then functionalized with biotin groups.[119,120] Due to possible interference of unreacted

biotin groups along the chain with subsequent interactions, it can be beneficial to functionalize the reducing end of the GAG instead.[121] For example, end-on biotinylated HA has been immobilized to both SLBs (section 4.1.1)[118] and SAMs (section 4.1.2)[122].

The interaction between biotin and SA was utilized in **Paper II, III & IV** for immobilization of biotinylated GAGs to SA-presenting SAMs.

4.2.4 Molecular adsorption and the layer-by-layer technique

Perhaps the easiest way to immobilize GAGs on surfaces is by the use of mere adsorption. For example, sulfated polysaccharides have been immobilized by solvent evaporation to wells used in enzyme-linked immunosorbent assay (ELISA).[123] Electrostatic interaction between the negatively charge GAG chains and a positively charged surface is commonly employed, e.g., heparin has been immobilized to glass surfaces carrying positive charges due to a coating of poly-L-lysine.[124]

By using a sufficiently high concentration of the immobilized GAG (or other charged polymers), the resulting surface charge upon adsorption is reversed, allowing for continued immobilization of oppositely charged polymers. The build-up of larger structures by alternately immobilizing polyionic and polycationic molecules (polyelectrolytes) with buffer washes in between, usually referred to as layer-by-layer assemblies, has been extensively used since the 90s (**Figure 10**).[125] It requires no special equipment and is compatible also with non-flat substrates, which often makes it a suitable approach for coating various biomaterials. The properties of the resulting assembly are defined by used polyelectrolytes (molecular weight, charge, stiffness), together with the pH and ionic strength of the solvent.[126-128] The growth of these films can be either linear or exponential, as a function of the number of layers. During exponential growth, a new deposition is proportional to the total film thickness, and occurs when one of the components diffuse in and out the film as the solvent is changed.[129,130] The high charge and high molecular weight make GAGs suitable for the LbL strategy and numerous examples can be found; e.g., HA and poly-L-lysine[129], CS and collagen[131] and heparin and chitosan[132]. A common application of these layers is to use them as cell-substrates, with or without the incorporation of various active biomolecules, e.g., growth factors (section 3.2.1).[67,132,133]
Layer-by-layer assemblies of heparin and chitosan were studied in **Paper V.**

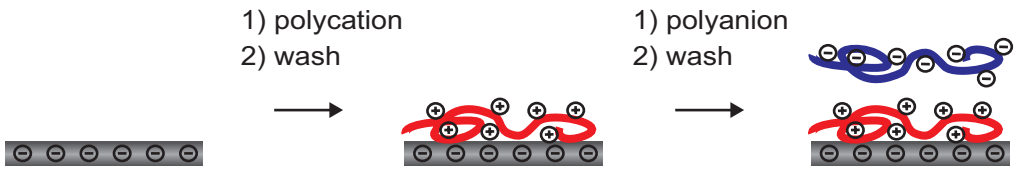

Figure 10. Formation of a polyelectrolyte multilayer via layer-by-layer assembly. Adapted from Decher et al. 1997.[134]

5

Studying glycosaminoglycan interactions

This chapter highlights some important aspects to consider when studying GAG-related interactions, complementing the ones listed in the previous chapter regarding a suitable immobilization of GAG to the surface, ensuring a retained biofunctionality.

5.1 Specificity

The resemblance in molecular structure between different GAG types, and the varying molecular structure within one GAG type (**Table 1**), raise the question of specificity in GAG-related interactions.[2,3,135] If a biomolecular interaction is *specific*, a biomolecule X reacts with, and only with, biomolecule A. For a non-specific interaction, where X can bind A, B, C, … a difference in *selectivity* (i.e. preference of binding) is seen. The thermodynamics of a system during an interaction is given by the Gibbs free energy:

$$\Delta G = \Delta H - T\Delta S \qquad Eq.\ 1$$

where ΔH is the change in enthalpy (the internal energy), ΔS is the change in entropy (the disorder), and T is the temperature of the system. An interaction occurs spontaneously if $\Delta G < 0$. Often for non-specific, spontaneous interactions, the primary contribution to the decrease in ΔG comes from an increase in entropy of the system.[136,137] For example, two hydrophobic entities in a water solvent are attracted to each other due to the increased disorder (ΔS) of water molecules upon binding. In the non-bound state, water molecules arrange around the hydrophobic entity, which is entropically unfavorable. Specificity in an interaction usually involves specific parts of the molecules, binding to one another in a directional manner. For example, a hydrogen atom bound to an electronegative atom (O, N) is attracted by other electronegative atoms (O, N or F) at short ranges. For such interactions, changes in enthalpy are usually significant. For GAG-protein interactions, hydrogen bonding can occur between the amino acids tyrosine, asparagine and glutamine and hydroxyl groups on the GAG.[3]

However, non-directional interactions can still render specificity in a correct 3D-arrangement of the two interacting partners. For example, the arrangements of positively charged, basic amino acids (lysine, arginine, histidine) have since long been suggested to be important in GAG-protein interactions, where a specific spacing between the amino acid side chains constitutes a GAG-binding region when the protein is correctly folded. The binding site on the protein surface should coincide with an appropriate charge distribution of the GAG chain, likely governed by the

sulfation pattern. This is often exemplified by the binding of heparin to antithrombin III (section 3.1).[35,138] A similar reasoning could be applied for hydrophobic amino acids (leucine and tyrosine) interacting with the N-acetyl group of the GAG.[3]

GAGs also posses secondary structures, as they adopt a helical structure in solution, stabilized by hydrogen bonds.[139,140] Also, the occurrence of kinks in the helix structure as well as *tertiary structures* where multiple GAG chains align in β-sheets, has been suggested to be important to render specificity in interactions.[141,142]

5.2 Multivalency

The affinity between a glycan structure and the glycan-binding site of a protein is generally low ($K_D \approx 10^{-3}$ M). In nature, high affinity interactions involving glycans is usually conveyed through *multivalency*, i.e. multiple recognition sites between two entities, e.g. when a virus binds to a cell or in cell-cell communication (**Figure 11a**).[143-145] Apart from giving rise to high affinity interactions, multivalent interactions *in vivo* are likely to allow control of interactions by other means, e.g. the spatial arrangement of receptors in a cell membrane.

Multivalency also has important implications when studying interactions using surface-based analytical techniques (**Figure 11b**). If the analyte has multiple binding epitopes, the response will be highly dependent on the ligand density on the surface and quantitative evaluation is difficult. In such cases, immobilization of the analyte is preferred.

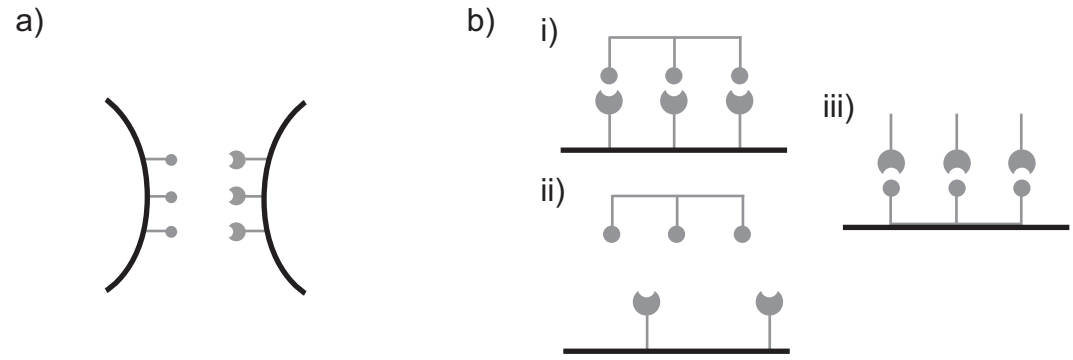

Figure 11. Schematic illustration of multivalency a) *in vivo*, exemplified by cell-cell communication, b) in surface-based sensing. In i) and ii), the binding of a multivalent analyte is measured, and binding is dependent on the ligand density on the surface. In iii), the same interaction is studied inversely, making the studied interaction monovalent.

5.3 Quantifying binding characteristics

For quantitative analysis of an interaction, binding constants are usually established. A simple biomolecular interaction can be represented by *Eq. 2*.

$$A + B \underset{k_\mathrm{d}}{\overset{k_\mathrm{a}}{\rightleftharpoons}} AB \qquad \textit{Eq. 2}$$

where A and B are two interacting molecules and k_a and k_d are the association and dissociation rate constants, respectively. The equilibrium association and dissociation constant can be defined as:

$$K_\mathrm{A} = \frac{[AB]}{[A][B]}, \quad K_\mathrm{D} = \frac{1}{K_\mathrm{A}} = \frac{[A][B]}{[AB]} \qquad \textit{Eq. 3}$$

Having the unit M, K_D is more often used when quantitatively describing an interaction, where a low value indicates an interaction of high affinity. If the interaction is studied using surface-based techniques, the binding of analyte A to ligand B can be related to the Langmuir adsorption isotherm, and the rate of change in surface coverage can then be described by:

$$\frac{d\theta}{dt} = k_\mathrm{a}[A](\theta_\mathrm{max} - \theta) - k_\mathrm{d}\theta \qquad \textit{Eq. 4}$$

where the first part represents association and the second part dissociation. θ is the surface coverage at time t and θ_max is the maximum surface coverage. At equilibrium, the rate of change, $d\theta/dt$ is zero, and solving for θ then gives:

$$\theta = \frac{[A]\theta_\mathrm{max}}{K_\mathrm{D} + [A]} \qquad \textit{Eq. 5}$$

where $K_\mathrm{D} = k_\mathrm{d}/k_\mathrm{a}$. Putting $[A] = K_\mathrm{D}$ gives $\theta = \theta_\mathrm{max}/2$, in other words, K_D equals the analyte bulk concentration at which half of the ligands on the surface are occupied. Also, by fitting the dissociation curve in order to get k_d, and by fitting the integral of *Eq. 4* to the association curve, K_D can be calculated by $k_\mathrm{d}/k_\mathrm{a}$.

Fitting measurement data to *Eq. 5* in order to get K_D is only reasonable if the Langmuir model holds, i.e. pure sample, homogenous surface with all sites equal and a non-cooperative binding. The presence of cooperativity in the interaction can be accounted for by extending *Eq. 5*, e.g., by: [146,147]

$$\theta = \frac{[A]^n\theta_\mathrm{max}}{K_{0.5}^n + [A]^n} \qquad \textit{Eq. 6}$$

where $n > 1$ indicates positive cooperativity. For $n = 1$, *Eq. 6* = *Eq. 5* and $K_{0.5} = K_D$.

6
Experimental techniques

6.1 Quartz Crystal Microbalance with Dissipation Monitoring

Quartz crystal microbalance with dissipation monitoring (QCM-D) is a mass-sensitive technique based on the oscillation of a quartz crystal. Quartz is a piezoelectric material, i.e., an electrical potential is developed when the material is subjected to mechanical stress. Conversely, a deformation of the crystal can be brought about if a potential is applied across the material. The mode of deformation is dependent on how the potential is applied relative to the crystal structure. In QCM techniques, an alternating potential is typically applied to a thin AT-cut single-crystalline disc with one gold electrode on each side, resulting in an oscillatory motion in the so-called *shear-thickness* mode (**Figure 12**).[148,149]

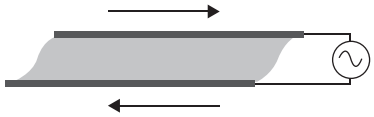

Figure 12. When an alternating potential is applied to an AT-cut quartz disc, it oscillates in a shear-thickness mode.

The most stable oscillation occurs at the resonance frequencies of the crystal, where a substantial part of the added energy is converted into motion. The fundamental resonance frequency can be described by:

$$f_0 = \frac{\sqrt{\mu_c \rho_c}}{2m_c} \qquad \textit{Eq. 7}$$

where m_c is the mass of the crystal, ρ_c is the density of the crystal, and μ_c is the shear elastic modulus of the crystal.[150] For common QCM crystal sensors f_0 = 5 MHz. If the frequency of the driving voltage matches the fundamental frequency of the crystal (or odd multiples of it), a standing wave is created in the crystal.[148] Adsorption of a biomolecule to the sensor surface typically leads to a decrease in the resonance frequency, since it is inversely proportional to the mass of the crystal sensor (*Eq. 7*, **Figure 13**). The sensing depth of the QCM technique is dependent on the extension of the shear oscillation into the solution, which in water is ~250 nm but increases with increased rigidity of the probed material.[151] As the measurement is based on mechanical oscillations, all mass that is acoustically coupled to the motion of the crystal sensor will be measured, i.e., including the solvent associated with the adsorbed molecules. Hence, the detected mass is the sum of the mass of the adsorbed layer and the mass of the associated solvent:

$$m = m_{layer} + m_{solvent} \qquad Eq.\ 8$$

By combining QCM with another technique that measures only m_{layer}, e.g., surface plasmon resonance-based techniques (SPR, section 6.2), the extent of hydration of the adsorbed layer can be estimated under the assumption that the modeled thicknesses, as well as other factors during the two experiments, are similar.[100,152]

Apart from measuring the change in frequency upon adsorption, the damping, or *dissipation*, is also measured by monitoring the time it takes for the oscillation to decay, τ, as the driving potential is switched off. During a measurement, the driving potential is continuously switched on and off, allowing a continuous measurement of the dissipation factor. The dissipation can be related to the energy stored and lost (dissipated) by[153]

$$D = \frac{1}{2\pi} \cdot \frac{E_{dissipated}}{E_{stored}} = \frac{1}{\pi f \tau} \qquad Eq.\ 9$$

where f is the resonance frequency and E_{stored} and $E_{\text{dissipated}}$, the stored and dissipated energy, respectively, during one oscillation period. For rigid films, the oscillation decays quickly and the dissipation is low. For soft, viscoelastic film, the dissipation is higher (**Figure 13**).

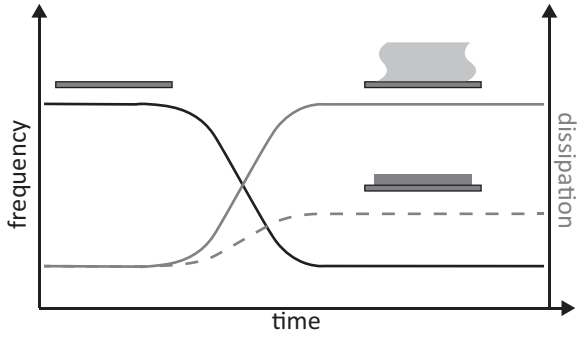

Figure 13. Illustrative QCM-D frequency and dissipation shifts describing adsorption of material. As material adsorbs, the resonance frequency (black) decreases and dissipation (light grey) increases. If the adsorbed layer is soft the dissipation response is large (solid), if it is dense, the dissipation response is small (dashed).

6.1.1 Modeling of QCM-D data

The simplest and most commonly used conversion of QCM-D frequency shifts to adsorbed mass is the Sauerbrey relation, which is derived from the resonance frequency of the quartz crystal sensor, *Eq. 7*:

$$\Delta m = -\frac{C\Delta f_n}{n} \qquad Eq.\ 10$$

were Δm is the change in mass, C is a crystal specific constant (17.7 ng/(cm^2·Hz)), n is the harmonic number and Δf_n the frequency change measured for that harmonic.[150,154] As seen from *Eq. 10*, the dissipation is not taken into account. The Sauerbrey equation hence only holds for thin, rigid layers displaying small dissipation shifts. As a rule of thumb, the Sauerbrey equation can be used if[153]

$$\frac{\Delta D_n}{\Delta f_n/n} \ll 0.4 \cdot 10^{-6} Hz^{-1} \qquad Eq.\ 11$$

This is often realized from that the frequency signal for the different harmonics overlap. Apart from this, the adsorbed layer should be tightly coupled to the sensor, evenly distributed, and $m_{\text{layer}} << m_{\text{c}}$.

When *Eq. 11*, or other requirements for the Sauerbrey equation do not hold, the Sauerbrey equation will give an underestimation of the mass, as the propagation of the standing wave then depends on the viscoelastic properties of the layer and the bulk liquid. A more elaborate physical model is then needed.[155,156] The dynamic shear modulus for a viscoelastic material can be described as

$$G = G' + iG'' \qquad Eq.\ 12$$

$$G' = \mu, \qquad G'' = \omega\eta \qquad Eq.\ 13$$

where ω is the angular frequency of the oscillation, μ the shear elastic modulus and η the shear viscosity. G' represents the elastic contribution and describes the energy stored, G'' represents the viscous contribution and describes the energy losses in the system.

Eq. 12 and *Eq. 13* are used to define the equation for the shear wave propagating in a viscoelastic medium. In terms of QCM-D experiments, some boundary conditions apply, e.g., the no-slip condition meaning that the adlayer on top of the sensor must be firmly attached and not slide during the oscillation. With the boundary conditions, the solution of the wave equation can be solved into expressions for Δf and ΔD depending on properties of the crystal sensor, the viscoelasticity of the adlayer and the viscoelastic contribution from the surrounding bulk liquid (**Figure 14**).[156] Δf also depends on the mass of the adlayers. In essence, the effect of measuring in a liquid environment emphasizes the viscoelastic properties of the adlayer, hence making it possible to measure them.[155]

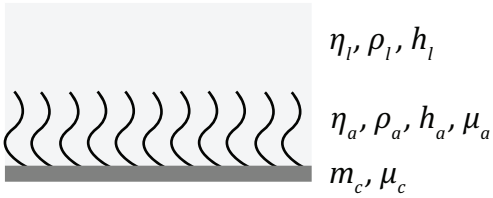

Figure 14. Shear elastic modulus μ, shear viscosity η, height h, mass m, and density ρ for a QCM-D crystal sensor c, carrying a viscoelastic adlayer a, in bulk liquid l.

In practice, when solving the wave equation for a particular experiment, properties of the crystal sensor and the liquid have to be known, and the density of the adlayer needs to be estimated. For a biological, soft layer, ρ_a = 1 g/cm^3 is often used. Even then, the equation leaves several unknown parameters, which can be solved by including data from several harmonics.

6.2 Surface Plasmon Resonance

Surface plasmon resonance, SPR, refers to an optical technique that aids detection of mass adsorption at a surface interface based on changes in the interfacial refractive index. A surface *plasmon* is a charge-density wave that can exist at the interface between two media where the dielectric constants are of opposite sign, e.g., between a free-electron metal (e.g. gold or silver) and a dielectric.[157,158] The surface plasmon can be excited by light that fulfills momentum matching, i.e., resonance conditions between the surface plasmon and the incoming light. The excitation conditions for surface plasmona are highly sensitive to changes at the interface where it propagates. When material with optical properties different from the bulk adsorbs to the metal surface, the resonance condition for the plasmon is changed.

To measure this phenomenon, a typical SPR instrument is usually built according to the Kretschmann configuration (**Figure 15**).[159] A glass prism is coated with a thin metal film, usually gold.[157] Plane-polarized light is applied through the prism such that it hits the interface at an angle larger than the critical angle, $\theta > \theta_c$, where total internal reflection occurs. Under these conditions, no light is transmitted through the gold film but an electrical field wave (the evanescent field) is created, having an intensity that decays exponentially from the surface into the ambient medium.

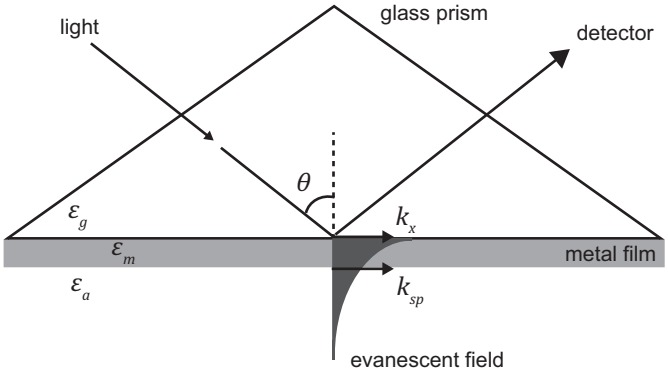

Figure 15. The Kretschmann configuration of an SPR instrument. k_x and k_{sp} are the wave vectors for the horizontal component of the light and the plasmon and ε_a, ε_m and ε_g are the dielectric constants for the ambient medium, the metal and the glass prism.

The wave vectors for the plasmon, k_{sp}, and for the parallel component of the incident light, k_x, are given by:

$$k_{sp} = \frac{\omega}{c}\sqrt{\frac{\varepsilon_m(\omega)\varepsilon_a}{\varepsilon_m(\omega)+\varepsilon_a}} = [|\varepsilon_m| \gg |\varepsilon_a|] = \frac{\omega}{c}\sqrt{\varepsilon_a} = \frac{\omega}{c}\, n_a \qquad \textit{Eq. 14}$$

$$k_x = \frac{\omega}{c}\sqrt{\varepsilon_g} sin\theta \qquad \textit{Eq. 15}$$

where ω is the angular frequency, c is the speed of light, ε_a, ε_m and ε_g are the dielectric constants for the ambient medium, the metal, and the glass prism, n_a is the refractive index of the ambient medium and θ is the incident angle of the light.[158] Note that $|\varepsilon_m| >> |\varepsilon_a|$ in *Eq. 14*, which is required for the plasmon to exist. For the plasmon and the light to be in resonance, k_x and k_{sp} need to be equal. Energy is then transferred from the light to the plasmon, causing a dip in the intensity of the reflected light sensed by a detector.[158,160] As molecules attach to the sensor surface, *Eq. 14* will change due to changes in the refractive index, n_a. In order for $k_{sp} = k_x$ to hold, the angle of incidence, θ, has to change. By scanning the incident angle until the resonance condition is found, the new refractive index, n_a, can be calculated.[157]

When communicating SPR data, the displacement of the resonance angle is sometimes reported. For the commonly used BIAcore instrument, values are often given in *resonance units* (*RU*). The *RU* values depend on the change in refractive index, Δn, which in turn is related to the surface concentration of the adsorbed biomolecule.[161] The change in mass, or surface coverage ng/cm^2, can be estimated using *Eq. 16*.[100]

$$\Delta m = \frac{C_{\mathrm{SPR}} \Delta RU}{\beta} \qquad Eq.\ 16$$

where C_{SPR} is a constant accounting for the decay length of the evanescent field, the sensitivity of the instrument and the refractive index increment for the adsorbed substance, dn/dC. β is a factor compensating for the distance from the sensing surface.

As opposed to the QCM-D technique (section 6.1), solvent associated with the adsorbed molecules is not measured, since it is only entities with a refractive index that is different from the surrounding solvent that is sensed. Measurements with SPR are often used to estimate affinity and kinetics for a given biomolecular interaction (section 5.3).

6.3 Fluorescence Recovery After Photobleaching

Fluorescence recovery after photobleaching (FRAP), is a microscopy method used to monitor the lateral diffusivity of fluorescently labelled molecules.[162] This can be useful for different kinds of systems, but a typical application is to monitor the mobility of lipids in a lipid bilayer (section 4.1.1). Apart from ensuring successful formation of a SLB, the technique can be used to probe changes in the fluidity due to an altered lipid composition or coupling of biomolecules to the lipid bilayer.[163] A fraction of fluorescently labelled lipids is incorporated into the SLB, and a small spot in the SLB is bleached by a high intensity light pulse. If the bilayer is fluid, the bleached and non-bleached lipids will diffuse and mix, and the fluorescence in the bleached spot will recover. By analyzing the recovery, the diffusion constant can be calculated.[164]

6.4 Isoelectric point analysis

The charge of a surface used in biomedical applications influence the immune complement system, blood coagulation and protein adsorption in general. It is therefore important in understanding the overall behavior of a material for the use in diagnostics, implants and as cell culture substrates. When a charged surface or particle is placed in an electrolyte, a charged double layer is formed close to the surface. The potential of this double layers, the zeta-potential or ζ-potential, can be used as an indicator of the surface charge.[165] For surfaces, this is commonly measured as a streaming potential or streaming current, by letting the surface under study constitute the walls of a narrow channel (~μm). When pushing an electrolyte through the channel, a fraction of the oppositely charged ions (opposite to the surface) is retained in the formed double layer. This violates the charge neutrality of the electrolyte and therefore a streaming current develops. The net stream of ions can be measured directly by electrodes on each end of the channel and the ζ-potential can be calculated by *Eq. 17*.[166]

$$\zeta = \frac{dI}{dp} \cdot \frac{\eta}{\varepsilon_0 \cdot \varepsilon_r} \cdot \frac{L}{A} \qquad \textit{Eq. 17}$$

where dI/dp is the slope of streaming current I versus the differential pressure across the sample p, η is the viscosity of the solution, ε_0 and ε_r is the vacuum permittivity and the relative permittivity for the electrolyte, L and A the length and cross-section area of the channel. The isoelectric point, i.e. the pH where the ζ-potential is zero, can be determined by measuring the ζ-potential during a pH titration.

6.5 Contact angle goniometry

The wetting property of a surface, i.e. if the surface is hydrophilic or hydrophobic, along with the surface charge (section 6.4), is an important property in determining the response from biological materials.[167] Wetting properties can be easily estimated by measuring the contact angle θ of a liquid, typically water, on the surface. The surface is considered hydrophilic if $\theta < 90°$, and hydrophobic if $\theta > 90°$ (**Figure 16**).[168] The contact angle depends on the interfacial energy between the three phases present: solid s, liquid l, vapor v, according to the Young's equation:[169]

$$\gamma_{sv} = \gamma_{sl} + \gamma_{lv} cos\theta \qquad \textit{Eq. 18}$$

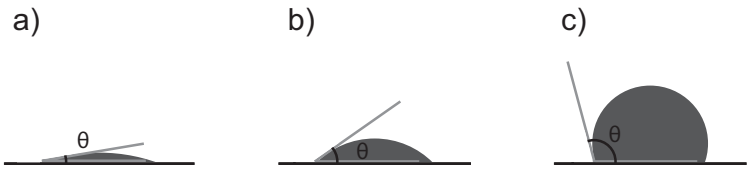

Figure 16. Contact angles for surfaces with different wettability; a) a super-hydrophilic surface with θ<10°, b) a hydrophilic surface with θ<90°, c) a hydrophobic surface with θ>90°.

The wetting properties of a surface depend on its surface energy. The surface energy can be considered as the energy needed to create a new surface from a bulk material, i.e. to break the chemical bonds in the bulk. To calculate the surface energy from the contact angle is not straight-forward and many models have been suggested.[170] A common approach is to measure contact angles of liquids having different surface tensions γ_{lv}, and plotting $\cos(\theta)$ versus γ_{lv}. The surface energy is then equal to the liquid surface tension γ_{lv} at $\cos(\theta) = 1$.[171]

7
Results

7.1 Summary of appended papers

The aim of this thesis project was to study GAG-related interactions with various biological entities (proteins, cells, viruses) in a reliable way using surface sensitive analytical techniques. A first step towards this is surface immobilization of GAGs, why this has been a major part. In line with this, the biofunctionality of the immobilized GAGs was assessed using different proteins. Based on these results, one strategy was chosen and used for further interaction studies.

In the first study, covalent immobilization of CS to SLBs was investigated via two strategies, either using naturally occurring carboxyl groups on CS, or using synthetically introduced hydrazide groups (**Paper I**). The results from this study emphasized the influence of introduced functional groups on the resulting biofunctionality of the immobilized GAGs. To investigate this further, and also how orientation of the GAGs influence protein interactions, HA and CS functionalized with biotin at the reducing end of the chain, as well as along the chain, were immobilized to a SA-presenting SAM (**Paper II**). A clear difference in the interaction with the GAG-degrading enzyme hyaluronidase was seen depending on the placement of biotin groups. The influence of the orientation of the immobilized GAG on the interaction between CS and the proteoglycan aggrecan was also studied. Based on these studies, end-on immobilization of GAGs using biotin-SA interactions was chosen as a suitable platform for further interaction studies. The platform was then used to study the interaction of gC, a glycoprotein isolation from HSV-1, with GAGs (**Paper III**). The results revealed important aspects regarding certain glycosylated structures on gC, by comparing binding between native gC and a mutant gC, lacking these glycosylated structures. The same platform was also used to study interactions with the growth factor BMP-2, as well as the initial binding of chondrocytes to hyaluronan (**Paper IV**), showing interesting effects from the cells on the underlying HA. In a separate study, the build-up of layer-by-layer structures consisting of heparin and chitosan was studied (**Paper V**).

7.2 Glycosaminoglycan library

The starting materials for the GAG derivatives used in this thesis work were obtained from commercial sources. In order to investigate different immobilization techniques, some GAGs were functionalized either via functional groups along the chain, or via the open form of the reducing end, presenting an aldehyde group (**Figure 7**, **Figure 17**). Some GAG derivatives were also sulfated. Functionalization and sulfation were carried out by our collaborators, INNOVENT (Jena, Germany). A full list of the GAGs used in the appended papers can be found in **Table 2**.

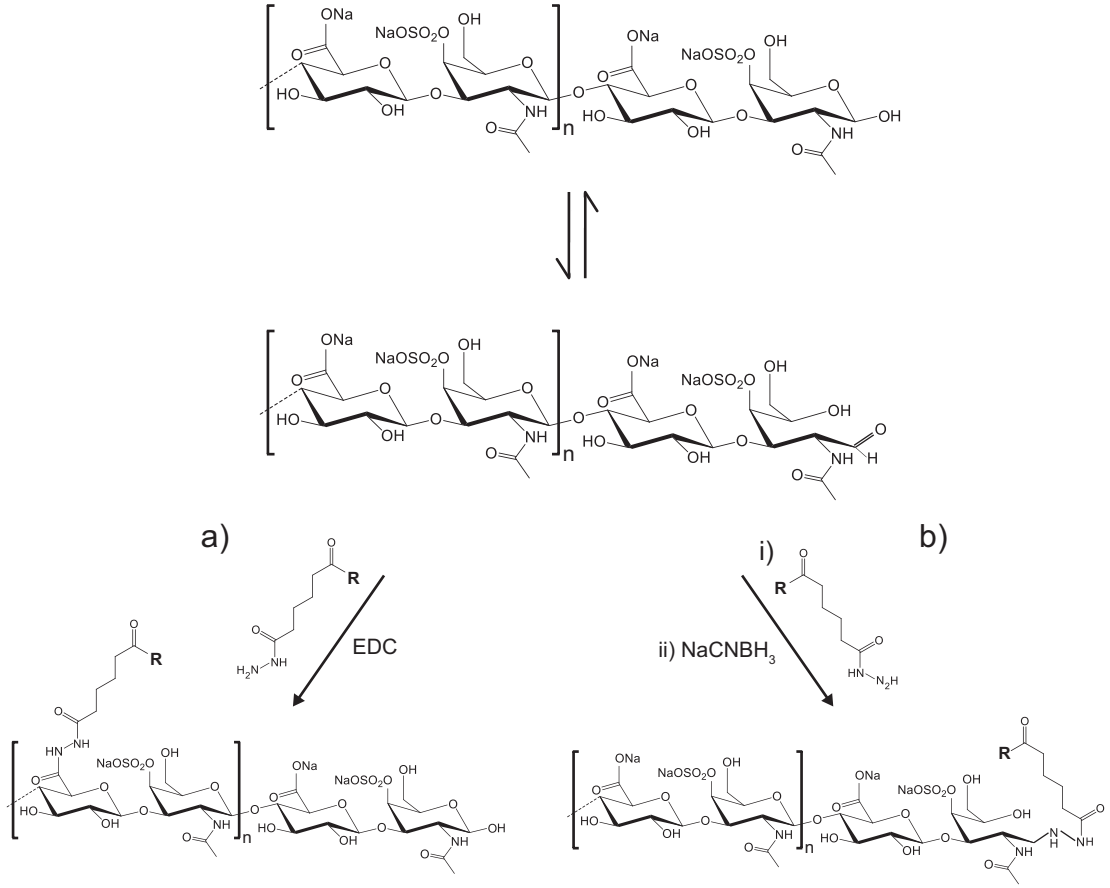

Figure 17. In the upper part of the figure, the molecular structure of a GAG (exemplified by CS) is shown, with the closed and the open structure of the reducing end. In the lower part of the figure, two strategies for the functionalization of CS by hydrazide reactions are exemplified: a) side-on functionalization via carboxyl groups along the GAG chain, and b) end-on functionalization to the aldehyde in the open structure of the reducing end. In Paper I, R=NH-NH_2 (hydrazide), in Paper II, R=C_4H_8-biotin

Table 2: GAG derivatives used in the thesis work.

	Abbreviation	Mw [kDa]	Functionalization[3]	$DS_{sulfate}$[3]	In paper
	CS	20	-	0.9	I
	h-CS 0.05	20	$DS_{hydrazide}$<0.05	0.9	I
	h-CS 0.2	20	$DS_{hydrazide}$=0.2	0.9	I
Chondroitin	**h-CS 0.4**	20	$DS_{hydrazide}$=0.4	0.9	I
Sulfate[1]	**b-CS**	20	end-on biotin	0.9	II, III
	b-CS 0.5%[2]	20	DS_{biotin}=0.53%[2]	0.9	II
	sCS	20	-	3.4[4]	II
	b-sCS 0.9%[2]	20	DS_{biotin}=0.88%[2]	3.4[4]	II
Hyaluronan	**HA**	1000	-	-	II
	HA	15	-	-	-
	b-HA	23	end-on biotin	-	II, III, IV
	b-HA 2.6%	1000	DS_{biotin}=2.6%	-	II
	b-HA 4.3%	90	DS_{biotin}=4.3%	-	II
	b-sHA	30	end-on biotin	3.1[4]	II, III
Heparin	**HS**	11	-	1	V
Chitosan	**CHI**	500	-	-	V

1: 70% CS-A, 30% CS-C

2: corrected values from those presented in Paper I

3: $DS_{hydrazide}$: average number of hydrazide substituents per repeating unit, DS_{biotin}: 100% indicates one biotin per repeating unit, $DS_{sulfate}$: average number of sulfate groups per repeating unit.

4: synthetically introduced sulfation

7.3 Strategies to immobilize glycosaminoglycans

7.3.1 Covalent immobilization to supported lipid bilayers (Paper I)

The immobilization of GAGs to SLBs (section 4.1.1) could be viewed as having two aims: i) developing strategies for more advanced cell membrane mimics by the addition of cell membrane GAGs, and ii) providing a good platform for GAG interaction studies when using surface-based analytical techniques as certain SLBs has proven to be good in minimizing non-specific interactions during biomolecular interaction studies.[99,172] In **Paper I**, the GAG CS was covalently attached to SLBs via two different strategies: either by activating the naturally occurring carboxyl groups on CS and coupling them to amine groups on the surface (**Figure 7a**), or by coupling activated carboxyl groups on the surface to hydrazide molecules introduced on CS (according to **Figure 7b** and **Figure 17a**, here termed h-CS). Both strategies were

followed in QCM-D. Accordingly, two different types of SLB were formed: one carboxyl-functionalized (SLB-COOH), and one amino-functionalized (SLB-NH_2) (**Figure 18**). Different ratios of the functionalized lipids were tried and SLB-COOH having a ratio of functional lipids up to 20% could be successfully formed. Formation of SLB-NH_2 was limited by the possibility to prepare a homogenous lipid mixture as lipid vesicles aggregated at a mole fraction of functionalized lipids >60%. The bilayer formation processes depend on the interaction between the charged head groups and the surface; a higher ratio of negatively charged lipid head groups aggravate/delay bilayer formation whereas the opposite is true when the ratio of positive lipid head groups is increased.

h-CS variants with different degrees of hydrazide functionalization were immobilized to SLB-COOH by activating the carboxyl groups on the surface by EDC/NHS reagents (section 4.2.2) (**Figure 19a**). Coupled amounts increased with increasing hydrazide functionalization and decreased with increasing ratio of functionalized head groups in the bilayer, likely due to a charged repulsion between the bilayer and the negatively charged CS chain. CS was also end-on functionalized with hydrazide but this did not lead to any detectable immobilized amounts on a SLB. As a second strategy, naturally occurring carboxyl groups on non-functionalized CS were activated in bulk, also by the use of EDC/NHS reagents, and coupled to SLB-NH_2 bilayers (**Figure 19b**). Immobilized amounts increased with increasing ration of functional lipids in the bilayer.

Both strategies resulted in thin layers of CS (25-55 ng/cm^2), immobilized in a side-on configuration. The viscoelastic properties were similar for layers obtain by the two strategies, as seen by similar $\Delta D/\Delta f$ ratios. The dynamic structure of SLBs could pose problems when immobilizing long chains or large structures as lipid material could potentially be removed.[118] Thus for comparison, h-CS was immobilized to SAM-COOH. Only small differences were seen when comparing the immobilized amount of CS to the SAM, suggesting that the fraction of DOPE-COOH lipids is a rather good measure of the number of carboxyl groups exposed at the surface and that the low response is not caused by removal of lipid material.

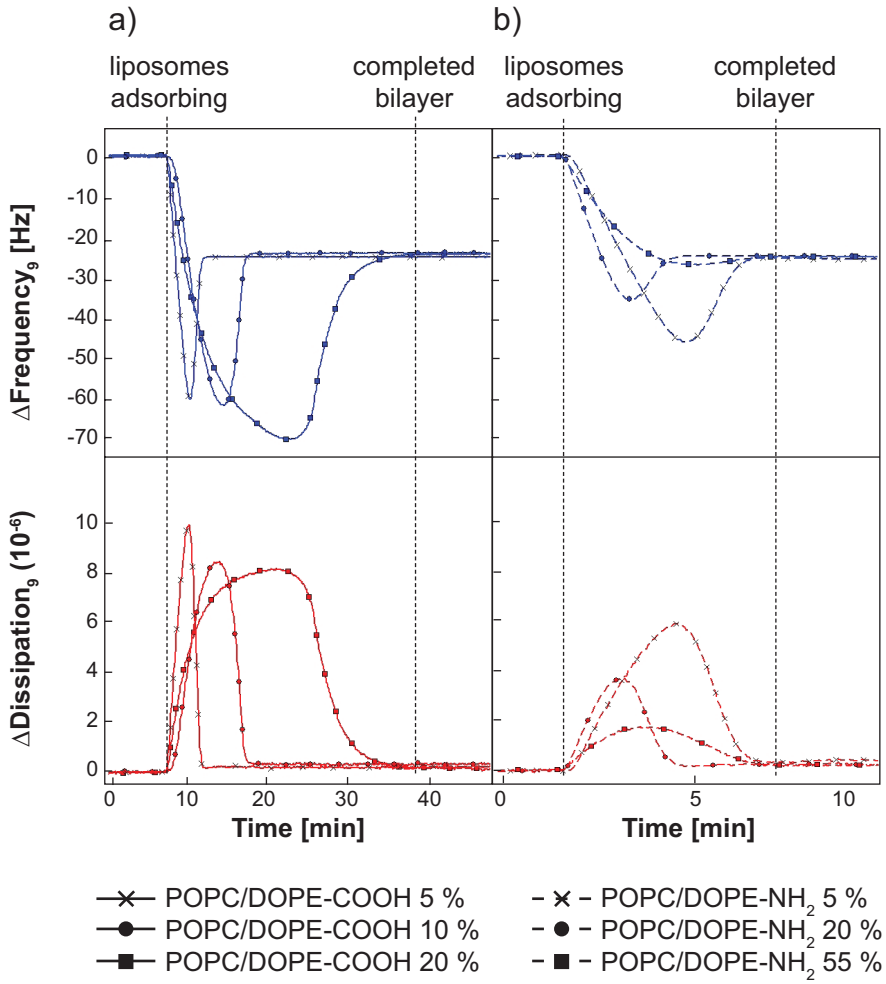

Figure 18. QCM-D frequency and dissipation shifts for the formation of a) SLB-COOH and b) SLB-NH_2 having different fractions of functionalized lipids.

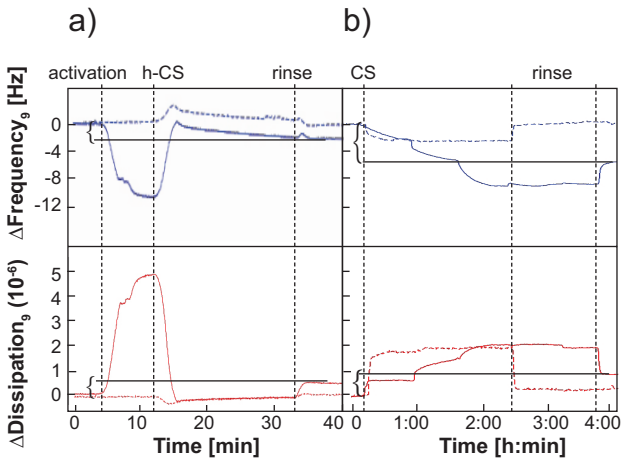

Figure 19. QCM-D frequency and dissipation shifts for the immobilizing of CS to SLBs. a) h-CS ($DS_{hydr.}$ 0.2) added to activated (solid line) and non-activated (dashed line) SLB-COOH 5%. b) stepwise addition of bulk activated CS to SLB-NH_2 5% (dashed line) and to SLB-NH_2 55% (solid line).

The lateral diffusion of lipids in the SLB was also assessed using fluorescence recovery after photobleaching (FRAP). The diffusion coefficient (D) of fluorescently labeled lipids was calculated, showing no significant difference between a functional bilayer and bilayer with immobilized CS. If the lipids in the bilayer have a retained fluidity, it is likely that the immobilized CS chain can adopt a relaxed configuration. $\Delta D/\Delta f$ ratios were in fact higher for h-CS immobilized on SLB-COOH compared to h-CS immobilized to a comparable SAM.

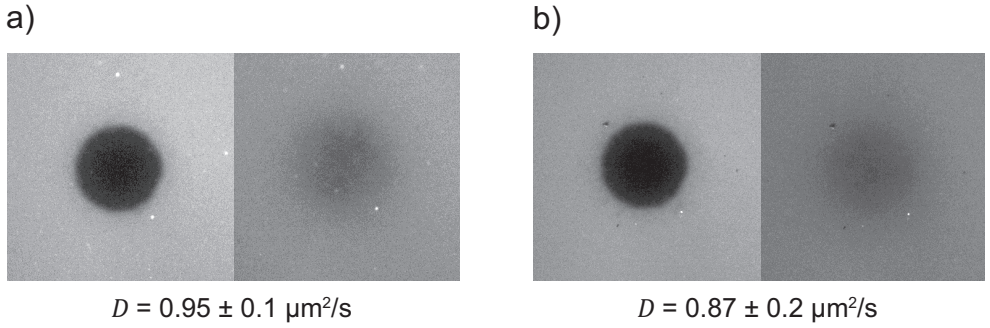

Figure 20. FRAP images of SLB-NH_2 20% containing 1% of fluorescently labeled lipid (NBD-POPC) a) without and b) with immobilized CS. After bleaching, 30 images were taken with a 5 s pause in between. The last image is shown to the right in each section.

7.3.2 Immobilization via biotin-streptavidin on self-assembled monolayers (Paper II-IV)

The immobilization of various biotinylated GAGs were made to a SA-presenting SAM (section 4.1.2 & 4.2.3). The SAM has been previously developed and characterized for QCM-D measurements, and consists of a mixture of disulfide OEGs (99% dS-OEG-OH + 1% dS-OEG-biotin).[105] The GAGs were primarily end-on biotinylated according to **Figure 17b**, but side-on biotinylation according **Figure 17a,** was also used. Immobilizations of end-on biotinylated chondroitin sulfate (b-CS), hyaluronan (b-HA) and sulfated hyaluronan (b-sHA) was monitored by QCM-D and SPR-based sensing (**Figure 7d, Figure 21**). Characteristics for the layers are summarized in **Table 3**.

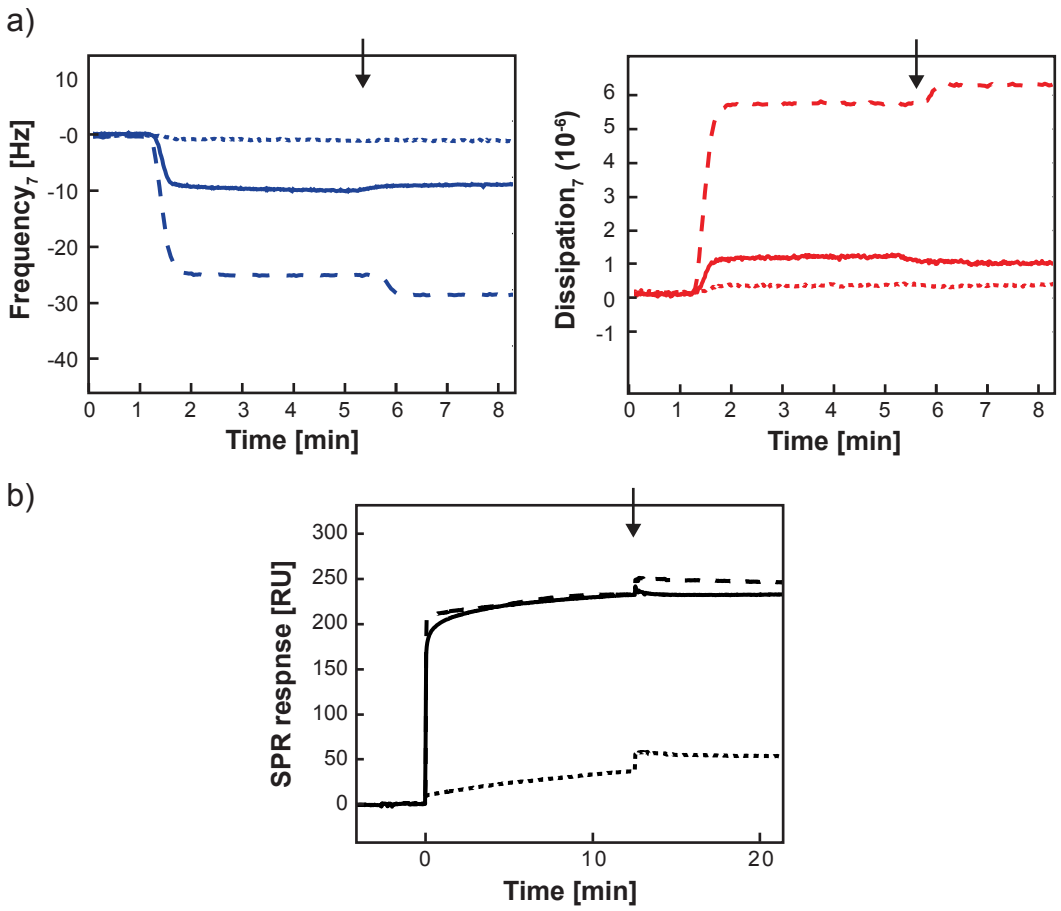

Figure 21. Immobilization of b-HA (dashed line), b-sHA (solid line) and b-CS (dotted line) to SA on a biotinylated OEG-SAM as monitored by a) QCM-D frequency and dissipation signals and b) SPR response. In order to reach saturation of b-CS multiple injections were needed (not shown). Arrows indicate rinsing.

Table 3. Physical and optical properties, along with measured masses and estimated water content of end-on immobilized GAGs.

	Mw [kDa]	$m_{QCM\text{-}D}$[a] [ng/cm^2]	m_{SPR}[b] [ng/cm^2]	**Chain-to-chain distance** [nm][c]	**hydration** [%]
b-HA	30	1080	20 ± 1	15 ± 3	98
b-CS	20	110	11 ± 2	19 ± 6	90
b-sHA	23	230	21 ± 2	17 ± 4	91

a: obtained through viscoelastic modeling, section 6.1.1.
b: calculated using Eq 16 and dn/dC from literature values[173-176], see supporting information of Paper II
c: assuming hexagonal close-packing

The degree of hydration estimated from these measurements are in good agreement with previously published data on HA.[118] The lower grafting density of b-CS could potentially be explained, despite careful purification by dialysis, by the presence of free biotin residues in the sample.

To further characterize the GAG layers, ζ-potential measurements and contact angle measurements were made (**Figure 22**).

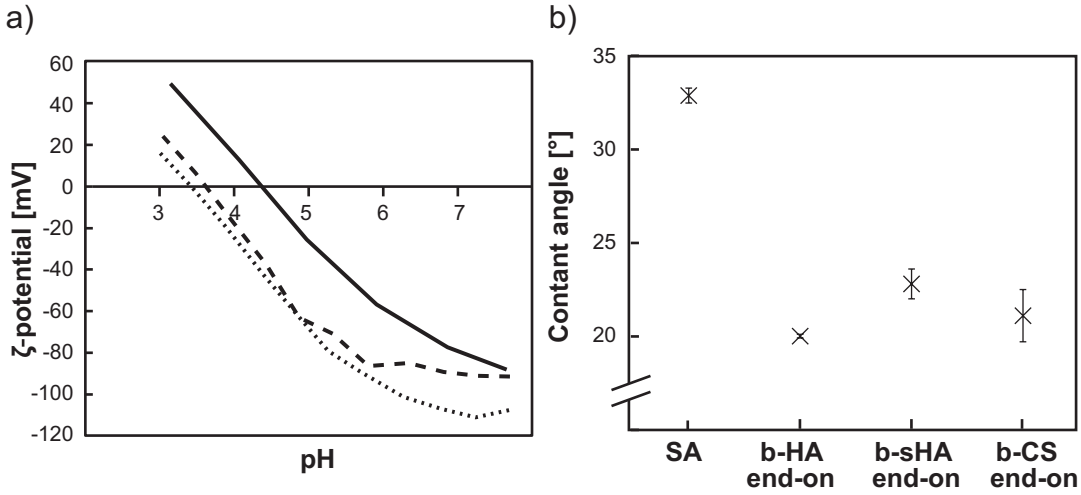

Figure 22. a) ζ-potential dependence on pH for SA (solid line), b-HA (dashed line), and b-sHA (dotted line). b) Water contact angles for surfaces displaying SA only, and SA with end-on immobilized GAGs.

No great differences between the GAG layers were measured using these techniques. The GAGs differ between one another primarily in terms of sulfation. For ζ-potential, the presence of sulfate groups is expected to lower the isoelectric point (ζ-potential at pH = 0) due to a higher charge of the polymer. The influence of sulfate groups on the wettability is less straightforward as both hydroxyl groups and sulfate groups are expected to yield a very hydrophilic polymer. Surface immobilization of HMW HA in a side-on configuration has previously shown to yield lower contact angles compared to CS immobilized in the same way, although generally more hydrophobic than the values seen in **Figure 22**b.[111] It is important to note that both the QCM-D and SPR results point to a difference in surface coverage between the GAG derivatives, leading to a different exposure of the underlying SA layer in each of the cases. There could therefore be an effect from the underlying SA layer, increasing the isoelectric point and the contact angle. Using longer GAG chains could reduce this effect and potentially show a greater difference between the derivatives.

The strategy of immobilizing GAGs via biotin-SA can obviously be used together with other surface modifications than a SAM, e.g., by including a fraction of biotinylated lipids into a SLB. The thiol-SAM used here is compatible with gold surfaces, which enables comparative experiments using of both QCM-D and SPR.

7.3.3 **Build-up of layer-by-layer structures** (Paper V)

In **Paper V**, characteristics of layer-by-layer structures (section 4.2.4) consisting of alternate layers of anionic heparin and cationic chitosan were investigated (**Figure 7a**). The chitosan solution was always applied at pH 4 but the pH of heparin was varied, as pH is known to affect the properties of a multilayer. This lead to three different assembly strategies (**Figure 23**); a) heparin applied at pH 4, b) heparin applied at pH 9, c) heparin applied at pH 4 up to the 7th layer and at pH 9 for the remaining layers. Among other techniques, the layer build-up was studied using QCM-D.

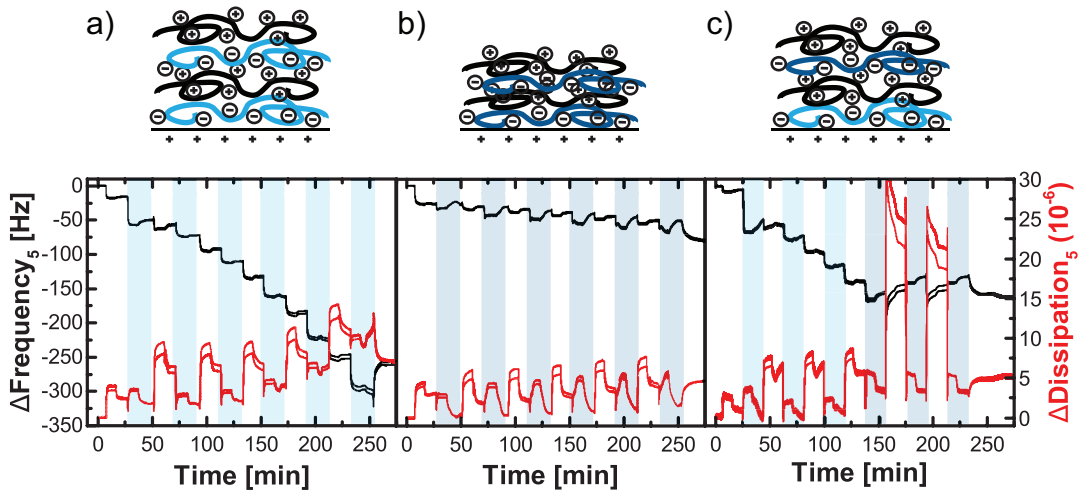

Figure 23. QCM-D frequency and dissipation signals for alternate additions of the anion heparin (blue) and the cation chitosan (black). 5th and 7th harmonic shown. Chitosan was applied at pH 4 at all times and heparin was applied at a) pH 4, b) pH 9 (dark blue), and c) pH 4 during the first three layers and pH 9 for the last three layers. Heparin addition (including rinsing) is marked by blue shading in the graph, light blue = pH 4, dark blue = pH 9.

The alteration in dissipation represents the change between swollen and condensed states of the multilayer; layers swell as chitosan is added, and condense as heparin is added. During strategy a) when heparin was applied at pH 4, ion paring is likely the dominating interaction between chitosan and heparin, as chitosan is positively charged at this pH. When heparin is applied at pH 9 according to strategy b), the underlying chitosan is non-protonated and ion pairing is hence not possible. The observed Δf is also smaller. It is interesting to note that the shift from pH 4 to pH 9 for the heparin solution in strategy c), causes a layer degradation during the addition of chitosan. This has been seen before for multilayer systems consisting of oligomers, like heparin used here.[177] Likely, the formation of soluble complexes is favored compared to adsorption to the surface. However not very apparent during strategy b), this is a likely mechanism for the limited layer growth seen. Also, the smaller heparin molecule is likely to diffuse in and out of the layer during build-up, especially at pH 9 when ion pairing is not extensive. This contributes to the some-what exponential growth seen,[129,130] and leads also to that the resulting structure does not consist of well-separated polymer sheets, but is a more intermingled structure.

Additional experiments using the layer-by-layer structures showed that adsorption of fibronectin, as well as cell attachment and spreading, was low on layers built according to strategy a), but higher to the denser layers formed using strategy b). Strategy c) resulted in improved cell attachment compared to layers formed using strategy a). At the same time, these layers are thicker than layers former using strategy c), which could allow for the incorporation of growth factors.

7.4 Biofunctionality of immobilized glycosaminoglycans

7.4.1 Influence of introduced functional groups (Paper I & II)

Many of the immobilizing strategies mentioned in section 4.2 include functionalization of the GAG with an active molecule of some sort. Introducing functional groups on the GAG could change its characteristics, and especially affect how it interacts with other biomolecules. This aspect was highlighted in **Paper I** and **II**.

In **Paper I**, the interaction between CS immobilized as described in section 7.3.1 and the growth factor bone morphogenetic protein-2 (BMP-2) was studied with QCM-D (**Figure 24**). The interactions between GAGs and growth factors are interesting to study because of the potential of combining the two in therapeutic applications to obtain an increased lifetime and stability of the growth factor (section 3.2.1). BMP-2 is frequently used in research, primarily with the aim of stimulating bone growth and regeneration.

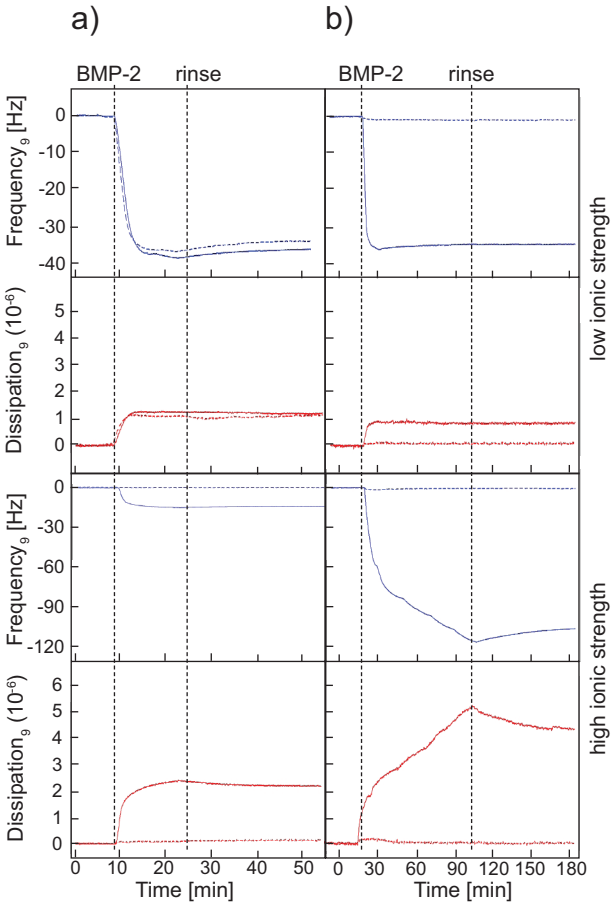

Figure 24. QCM-D frequency and dissipation signals when adding BMP-2 to a) h-CS immobilized to SLB-COOH 5% and b) CS immobilized to SLB-NH_2 20% (solid lines) and to SLBs without immobilized CS (dashed lines). Addition was made in low (top) and high (bottom) ionic strength acetate buffer. After addition, the system was rinsed with the acetate buffer just used (indicated in the graph), and later with PBS (not shown).

In low ionic strength buffer there is no difference between BMP-2 binding to CS or to the negatively charged SLB-COOH. Increasing the ionic strength displays a lower but presumably more specific interaction between h-CS and BMP-2. When using the positively charged SLB-NH_2, there is no non-specific interaction (independent of the ionic strength) as the positively charged BMP-2 is rather repelled. Higher amounts of BMP-2 bound to CS immobilized on SLB-NH_2 (**Figure 24b**) compared to h-CS immobilized on SLB-COOH (**Figure 24a**) at high ionic strength. This can in part be due to that the added mass of CS when using strategy b) is about double as compared to strategy a, but more importantly CS is here expected to be more in its native form, as it has not been functionalized with hydrazide. Structural rearrangements are likely to occur as BMP-2 interacts with CS, and the reaction did not reach equilibrium during the used conditions. The appearance could also be due to an aggregation of BMP-2 induced at the sensor surface, but this was not seen for BMP-2 interacting with h-CS during the same conditions. Two binding sites on BMP-2 for the GAG heparin have been suggested[178] and a similar interaction with CS could be likely. For other GAG-proteins systems, like HA and the dimer TSG-6, a cross-linking behavior

has been seen.[122] Whether the interaction between BMP-2 and CS is of a cross-linking nature or if the CS chain accommodates itself in a binding pocket of BMP-2[179] is too early to say.

The effect of introduced functional groups on GAGs on protein interactions was further investigated in **Paper II**. The GAGs CS and HA, having biotin groups differently placed on the chains, were immobilized to a SA-presenting SAM (section 7.3.2) and degradation caused by the enzyme hyaluronidase was studies using QCM-D.

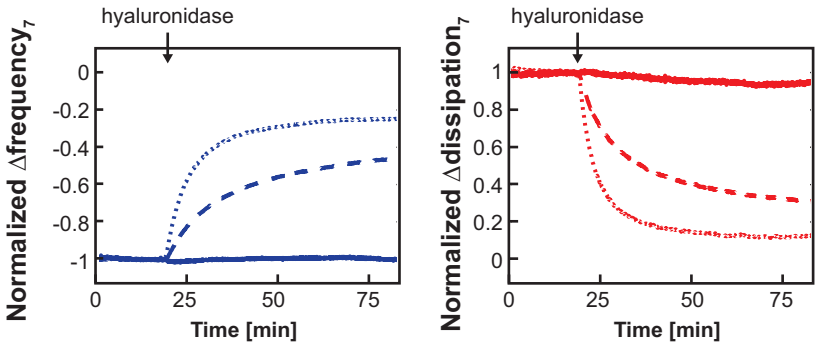

Figure 25. Normalized QCM-D frequency and dissipation signals when adding hyaluronidase I (pH 5.8) to biotinylated HA immobilized to a SA-SAM, b-HA 4.3% (solid line), b-HA 2.6% (dashed line) and b-HA end-on (dotted line). Degradation is seen as an increase in frequency and a decrease in dissipation. After the addition of hyaluronidase I the flow was stopped for 1 h with 2–3 intermediate pulses to introduce fresh enzyme.

When biotinylation was made side-on, along the HA chain, HA was not properly recognized by hyaluronidase and a low degradation was seen. The degradation decreased as the degree of biotinylation increased. However, end-on biotinylated HA was degraded to about 80% (**Figure 25**). The surface-based experiments were compared to bulk degradation of the same derivatives by hyaluronidase, studied using high performance liquid chromatography (HPLC). The results were the same, showing that the differences between the GAG derivatives are in fact due to functionalization rather than to surface immobilization.

Hyaluronidase could serve as a cheap probe to evaluate biofunctionality of surface immobilized GAGs before using more expensive proteins. Obviously, the relevance will depend on where on the GAG this protein is expected to bind. Hyaluronidase cleaves the β-1,4-glycosidic bond in HA and CS under acidic conditions, yielding tetra-or hexasaccharide products.[180-182] For side-on biotinylated derivatives, biotin groups are present on the carboxylic group on C6', close to the β-1,4-glycosidic bond, likely obstructing the action of hyaluronidase (**Table 1**).

An example of a GAG interaction resulting in larger supramolecular structures is the interaction between HA and aggrecan, illustrated in **Figure 1**. Aggrecan is a large

proteoglycan (~2.75 MDa[183]) consisting of a protein core with numerous CS and KS chains extending from it in a bottle-brush structure. Multiple aggrecan molecules can bind along the side of HA together with a link protein, building highly hydrated assemblies that are important for the pressure resistance of cartilage.[44] Here, the interaction between HA and aggrecan was studied using the QCM-D technique, experiments that also emphasized the influence of GAG-biotinylation. HA was either biotinylated along the HA chain and immobilized to an SA-SAM (section 7.3.2), or left non-functionalized and immobilized to a SLB-NH_2 (section 7.3.1). Aggrecan binding was higher to non-functionalized HA and low binding was seen to biotinylated HA (**Figure 26**). Since the amount of surface-bound HA depended on the immobilization method, aggrecan binding was normalized to the extent of HA immobilization. Saturation of the HA-surface was not reached with the experimental conditions used here, but values were taken after 10 min of aggrecan binding.

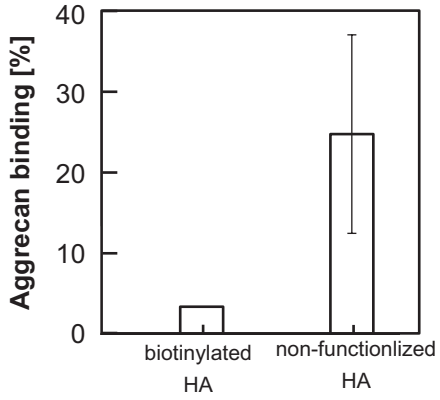

Figure 26. Normalized QCM-D frequency response after 10 min of aggrecan binding (10 µg/ml in PBS pH 7.4) to biotinylated HA (HA 4.3%) side-on immobilized to a SA-SAM and to non-functionalized HA side-on immobilized to SLB-NH_2 55%.

7.4.2 Side-on vs. end-on immobilization (Paper II, additional results)

The interaction between HA and aggrecan, mentioned above, also highlighted the influence of the configuration of the GAG on the surface, apart from the presence of functional groups. Although an end-on configuration of GAGs seemed like a promising strategy, the binding of aggrecan was hardly detectable to HA immobilized in this way, compared to when non-functionalized HA was immobilized in a side-on configuration (**Figure 27**, **Figure 28**).

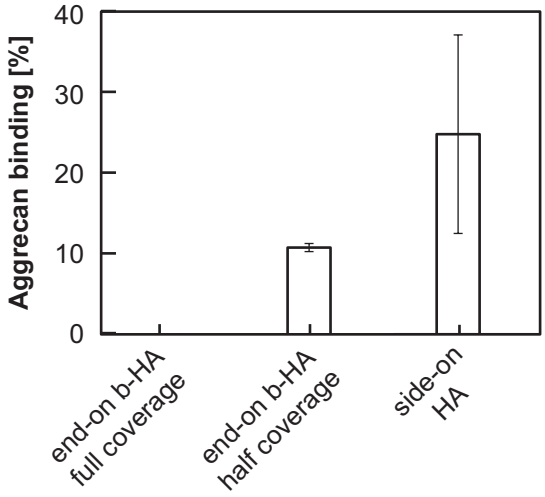

Figure 27. Normalized QCM-D frequency response after 10 min of aggrecan binding (10ug/ml in PBS pH 7.4) to end-on biotinylated HA (b-HA) displaying full or half coverage, biotinylated HA (HA 4.3%) side-on immobilized to a SA-SAM and to non-functionalized HA side-on immobilized to SLB-NH_2 55%. The rightmost bar is repeated from **Figure 26**.

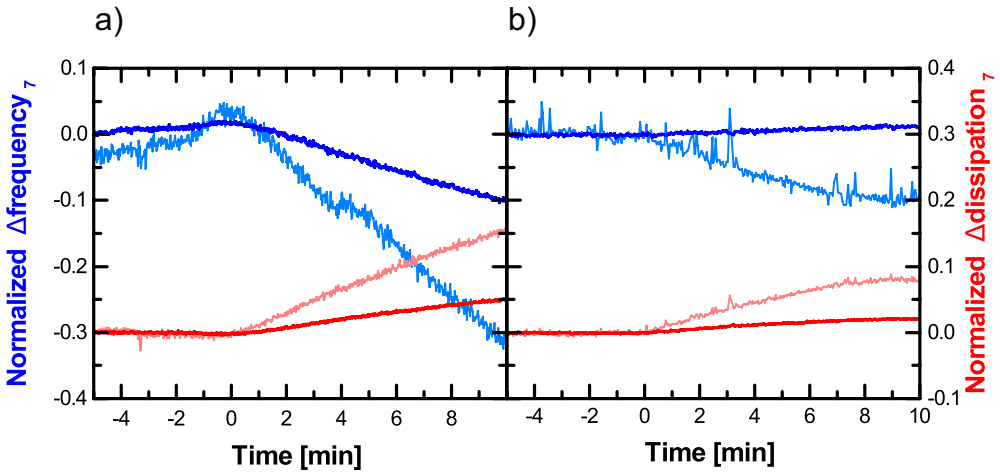

Figure 28. QCM-D frequency (blue) and dissipation (red) signals for a 10 min addition of aggrecan (10 µg/ml in PBS pH 7.4) to a) non-functionalized HA side-on immobilized to SLB-NH_2 55% and b) end-on biotinylated HA (b-HA) immobilized to SAM-SA (full coverage). The responses are shown for both the 1st (lighter colours) and 7th (darker colours) harmonic. The QCM-D response is normalized to the QCM-D frequency response for HA: 18 and 28 Hz, respectively.

However, several factors have to be taken into consideration when viewing these results. The HA chains used here are very short compared to HA in vivo (15-23 kDa compared to a few million Da), forming a, in comparison, closed-packed structure when immobilized in the end-on configuration. Based on measurements in SPR, a saturated surface of b-HA has a chain-to-chain distance of ~14 nm (**Table 3**). The CS chains of aggrecan extends ~30 nm out from the core protein,[184] hence the chain-to-chain distance is not enough to accommodate aggrecan in between the chains.

A lower coverage increased the binding but even here the chain-to-chain distance (~30 nm) is smaller than the width of aggrecan. However, similar responses to the ones seen in **Figure 28** have been reported recently, even though longer b-HA chains (~1 MDa) having a lower surfaces density, as well as a higher aggrecan concentration, were used.[185] As multiple copies of aggrecan can bind to the side of the HA chain, the side-on configuration of HA likely presents the molecules in a more accessible configuration. Aggrecan is a very large molecule, having a length of ~350 nm.[184] The sensing depths of QCM-D is ~250 nm in water,[151,186] hence, even a monolayer of aggrecan molecules in an end-on configuration on the QCM-D sensor, could partly extend outside the sensing depth and could be an additional explanation to the low values seen. It is interesting to note that *in vivo*, aggrecan molecules are likely packed very densely along the HA chain; measurements of 1 aggrecan molecule per 30 nm (on average) have been reported.[44]

7.5 Biological applications of surface immobilized glycosaminoglycans

7.5.1 Binding of herpes simplex virus glycoprotein C (Paper III)

As discussed in section 3.3, many viruses use GAGs on proteoglycans on cell surfaces as attachment factors to enable viral entry into to the cell and eventually spreading of the virus. For example, glycoprotein C (gC) on the herpes simplex virus (HSV) is known to interact with sulfated GAGs.[74,75] This glycoprotein, as well as other GAG-binding glycoproteins, has a mucin-like region rich in glycosylation (**Figure 29**). This region is known to be important in regulating the immune response from the host cell, as they either cause recognition or evasion of the virus from the immune system.[187-189] Less is however known about how this region influences the binding of viral glycoproteins to GAGs. In **Paper III**, we investigated how native HSV gC differed in its binding to sulfated GAGs, compared to a mutated version, gCΔmuc[85] that lacked the mucin-like region (**Figure 29**).

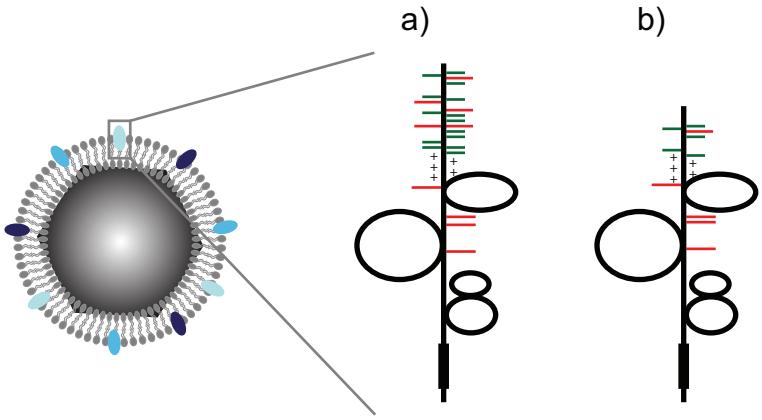

Figure 29. Schematic illustration of a HSV virion and a) native gC and b) the mutated version gCΔmuc. The gC includes a transmembrane region (bottom), loops caused by disulfide bridges, a positively charged GAG-binding region close to the mucin-like region consisting of numerous N-glycans (red) and O-linked glycans (green).

Binding of the two gC variants to non-sulfated b-HA, naturally sulfated b-CS, and synthetically sulfated b-sHA (**Table 2**) were probed using SPR-based sensing. Equilibrium binding curves were fitted to *Eq. 6* to obtain binding parameters (**Figure 30**).

a)

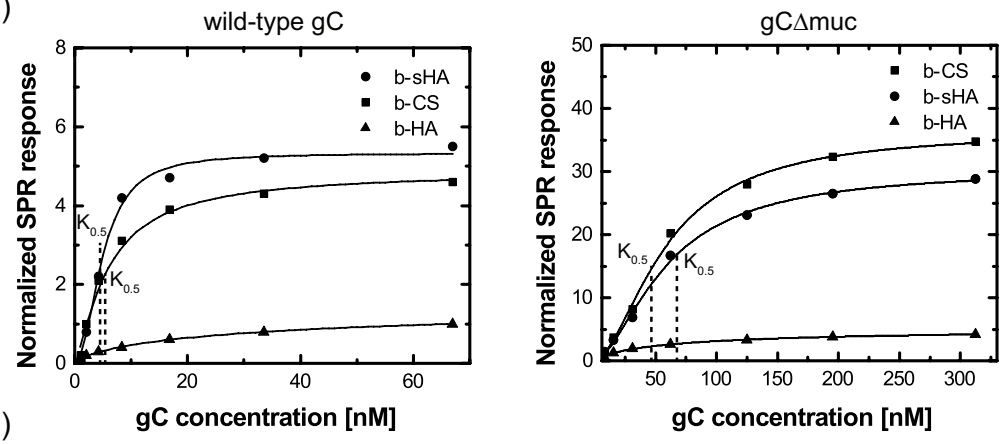

b)

GAG	$K_{0.5}$ [nM]		n		no. of gC/GAG	
	gC(KOSc)	gC(AC1)	gC(KOSc)	gC(AC1)	gC(KOSc)	gC(AC1)
CS	5.3 ± 0.6	47.7 ± 11.2	1 ± 0.5	1.6 ± 0.1	1.0 ± 0.4	16.5 ± 5.8
sHA	4.9 ± 0.04	66.3 ± 10.1	1.9 ± 0.3	1.9 ± 0.4	1.5 ± 0.3	14.6 ± 2.7

Figure 30. a) Representative equilibrium binding curves (symbols) fitted to Eq. 6 (lines) for native gC and gCΔmuc. The binding is normalized to the SPR response of GAGs on the surface. b) Binding parameters from the fitted curves in a).

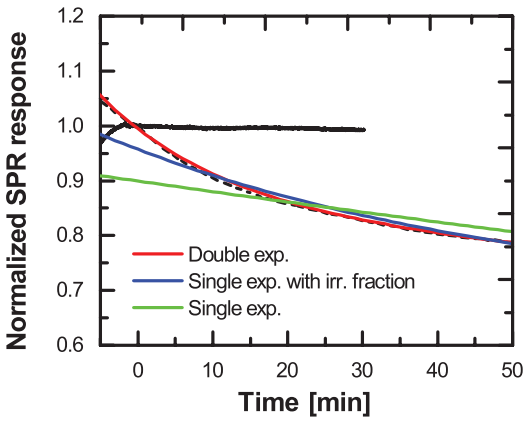

Figure 31. Normalized dissociation of native gC (dashed curve) and gCΔmuc (solid curve) from b-CS. A double exponential equation was required for a good fit of the native gC dissociation.

As expected, gCs bound preferably to the sulfated GAGs b-CS and b-sHA compared to non-sulfated b-HA. gCΔmuc, where the mucin-like region is deleted, had a lower affinity for the sulfated GAGs (**Figure 30**). However it also exhibited a slower dissociation (**Figure 31**), indicating that once formed, the interaction between gCΔmuc and sulfated GAGs is more stable than for native gC. The number of gC proteins that bound per GAG chain, calculated from the maximal gC binding estimated from *Eq. 6*, was significantly higher for gCΔmuc compared to native gC. Without the negatively charged mucin-like region, the gC is smaller and there is likely less repulsion between the gC and the GAGs as well as between gC copies, allowing them to pack more closely.

Interestingly, there was no significant difference between the two sulfated GAGs b-CS and b-sHA for either gC variant. CS and sHA differ in length, degree of sulfation and surface density (**Table 2**, **Table 3**) resulting in an order of magnitude higher surface density of sulfate groups. The synthetic sulfation of b-sHA occurs randomly whereas b-CS (CS-A/CS-C) has a more defined pattern (**Table 1**). This suggests that the positioning of sulfation groups on the disaccharide or along the GAG chain, rather than mere presence, is important in promoting gC binding. Also, the need for disulfated repeating units as a requirement for gC binding, which has been suggested by others,[190] was not supported in this study, as b-CS has no disulfated units.

In **Paper III**, the observation from the gC-binding studies was compared to cell studies with two virus strains carrying the different gC, KOS and KOS-gCΔmuc respectively. It was seen that KOS-gCΔmuc had a lower affinity to heparin and a shorter GAG-mimetic. Also, KOS-gCΔmuc particles seemed to be trapped on the surface of the cells. These results together suggest that the mucin-like region is not required for binding but rather has a modulating function, enabling release of the gC from the GAG and potentially also the virus from the cell surface. A tuned binding, but also unbinding, of viruses to cells is crucial for an efficient infectious cycle in order to avoid non-productive binding events where the virus is trapped instead of infecting the cell.

7.5.2 **Initial effect of chondrocytes** (Paper IV)

As discussed in section 3.2.4, HA is a common starting material for the construction of tissue scaffolds, used in, e.g., bone and cartilage applications. In **Paper IV**, human derived chondrocytes were added in serum-free media to b-HA immobilized to a SA-presenting SAM (section 7.3.2). The response from the added cells was studied under stagnant conditions for ~140 min before rinsing, using the QCM-D technique combined with light microscopy. As opposed to when adding chondrocytes to polystyrene (**Figure 32**, grey line), a commonly used cell culture material, addition of chondrocytes to b-HA induced an increase in frequency and a decrease in dissipation, indicating loss of material (**Figure 32**, black line). Light microscopy images taken of the b-HA modified surface show present, but non-attached chondrocytes, which are removed upon rinsing. In the case of polystyrene, attachment was observed. The combined results from the two techniques suggest that the chondrocytes do not bind to the b-HA, but rather that the GAG layer may be degraded in the presence of the chondrocytes, most likely by released enzymes. The change in the frequency and dissipation signals corresponds to ~90% of the signals for the HA-layer, and indicates a degradation comparable to that seen for hyaluronidase in **Paper II**.

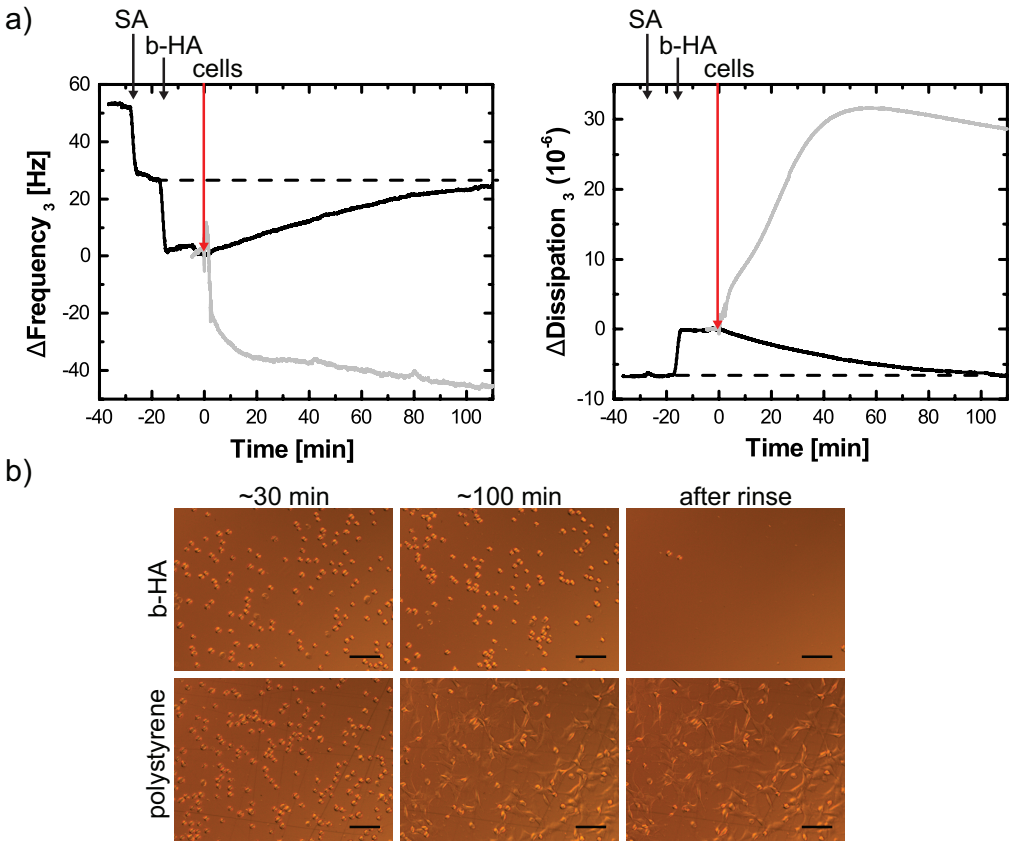

Figure 32. a) QCM-D frequency and dissipation signals for the addition of chondrocytes to polystyrene (grey) or to b-HA immobilized on a SA-presenting SAM (black). Addition of cells on both surfaces is set to zero, marked by a red arrow. Black arrows mark the prior additions of SA and b-HA. b) light microscopy images taken during the QCM-D experiment for the two surfaces at given time points. Scale bar is 100 μm.

The degradation response is fast, suggesting that the active substance is already present at the cell surface, or within the cell and released upon contact. One should note that the underlying HA-layer is expected to be very thin compared to the size of the chondrocyte (HA length ~60 nm vs. cell ∅ ~20 μm), and markedly different from, e.g., a HA-based scaffold, usually consisting of longer chains with extensive functionalization and/or crosslinking (section 3.2.4).

The occurrence of HA in cartilage *in vivo* is regulated by the expression of synthesizing enzymes (HA synthase) and degrading enzymes (hyaluronidases).[51] The primary route of HA degradation by chondrocytes occurs via CD44-mediated endocytosis, and later degradation in lysosomes within the cell.[191] However, the occurrence of lower molecular weight HA in the ECM suggests the presence of an extracellular degradation of HA as well.[51] The internalization of HA for degradation has been shown to be dependent of the molecular weight of HA; large HA molecules, or HA associated with aggrecan seems too large to be endocytosed.[192] It is easy to see how extracellular and lysosomal degradation could work in concert, degrading larger and smaller HA molecules and assemblies, respectively. An enzyme similar to PH-20, which is a membrane associated hyaluronidase active at neutral pH, has been found to be expressed and secreted by chondrocytes,[193] and might be a candidate for the effect seen here.

Even though additional experiments would be required to draw more precise biological conclusions, the study shows that the combination of QCM-D and light microscopy can be used to monitor changes in the interface between a material surface and a cell, even in the absence of cell attachment. The QCM-D technique is increasingly used in cell research, studying attachment as well as conformational changes.[194-198]

7.5.3 Interactions with bone morphogenetic protein 2 (additional results)

As discussed in section 3.2.1, the growth factor bone morphogenetic protein 2 (BMP-2) binds to GAGs, which could potentially offer a strategy to modulate the effect of BMP-2 *in vitro* and *in vivo*. However, both inhibitory[199,200] and promoting[178,201,202] effects of GAGs on BMP-2 interactions and cell-signaling has been presented in the literature. Hence the mechanisms behind the effect of GAG-growth factor binding are not fully understood. It is likely to be dependent on many factors, such as GAG length and sulfation pattern, as well as administered dosage and timing.

To complement the results in **Paper I**, where the binding of BMP-2 to side-on immobilized CS was studied, the same interaction was probed using end-on immobilized GAGs (section 7.3.2). Preliminary results are summarized in **Figure 33**.

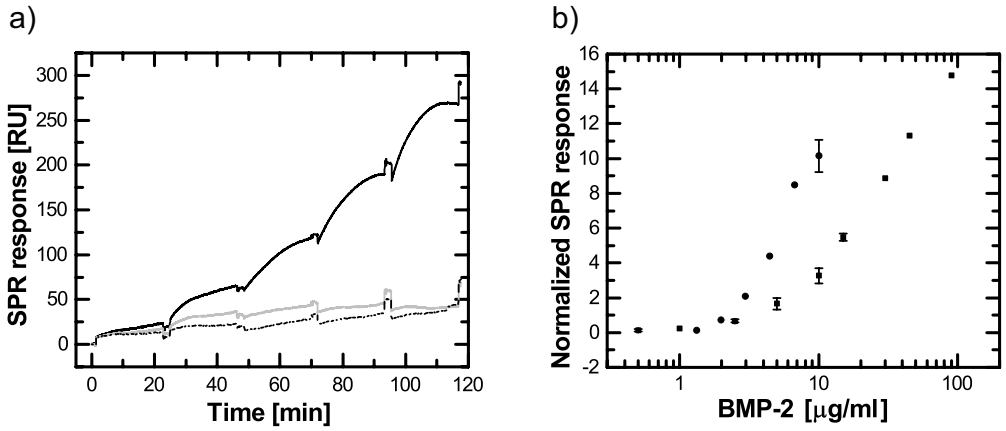

Figure 33. a) Example SPR curves showing binding of rhBMP-2 (in PBS at pH 7.4, using a series of concentrations; 0.5, 2.5, 5, 10, and 15 μg/mL) to immobilized b-CS (solid) and b-HA (dashed) as well as to the SA background (grey). b) The corresponding saturation values obtained for immobilized b-CS (squares, n=2 for the lower concentrations) and b-sHA (circles, n=2 for the highest concentration). The SPR responses are normalized to the SPR response for the corresponding GAG-layer.

Significant binding was only seen to the sulfated GAGs b-CS and b-sHA; the binding to non-sulfated b-HA was as low as to the SA background, which emphasize the importance of sulfation in this interaction. Although not complete at this stage, equilibrium binding curves suggest a higher affinity of BMP-2 to b-sHA (**Figure 33**b), which is in line with other studies where an increased degree of sulfation induced higher affinity for the binding growth factors BMP-2[199] and BMP-4[29]. However, in contrast to the mentioned studies, significant binding was seen already to the lower sulfated b-CS in our experiments (b-CS: $DS_{sulfate}$=0.9 vs. b-sHA: $DS_{sulfate}$=3.1, **Table 2**). This suggests a possible importance of sulfation of the C6 position, as this is partially sulfated in b-CS, and fully sulfated in b-sHA (**Table 1**).[29,201]

The affinity that can be expected from the curves in **Figure 33** is significantly smaller than what was reported previously for binding of BMP-2 to surface-immobilized heparin during physiological conditions (0.5 μg/mL or 20 nM).[178] This could be due to a difference in the BMP-2 batches or in the immobilization. In the mentioned study, a stoichiometric ratio of 5-6 BMP-2 molecules/ heparin chain (16 kDa) was estimated at maximal saturation (at 5 μg/mL (200 nM)). In our study, the highest stoichiometric ratio measured was 9 BMP-2 molecules/ b-CS chain at 90 μg/mL (3.5 μM). The fact that b-CS is 25% longer than the heparin used could explain why more BMP-2 proteins were accommodated. However, the solubility of BMP-2 is likely affected at these high concentrations, hence these values should be interpreted with caution. The grafting density of GAGs on the surface was not varied in our experiments, but is likely to have an effect on the number of BMP-2 molecules than could bind along one GAG chain. The grafting density used here (~20 nm between immobilized GAGs) should leave space for the homodimeric BMP-2 molecule (7x3.5x2.5 nm) as suggested by molecular modeling.[179]

The low binding seen to SA and b-HA was confirmed in measurements using the QCM-D technique. Furthermore, binding of BMP-2 to b-CS and b-sHA seemed to result in a condensation of the layers, as the $\Delta D/\Delta f$ ratio decreased when the growth factor was added. This is in line with what was seen for BMP-2 binding to h-CS immobilized in a side-on configuration in **Paper I** (section 7.4.1).

"Perspective should be something
you could buy on a bottle
and inject intravenously"

Erlend Loe. *Naïve. Super.*

8
Perspectives and outlook

The aim of this thesis project was to study GAG-related interactions using surface-based analytical techniques. This approach relies on controlled immobilization of GAGs to surfaces. It is important to note that to study how GAGs alone participate in an interaction is a simplification from the *in vivo* state, as most GAGs are linked to a proteoglycan core protein. Although an interesting strategy, immobilization of a whole proteoglycan would increase the potential variations in the molecular structure greatly. The strategy chosen here allows for detailed studies of how GAGs with different properties interact with various entities, rendering information that would likely be obscured in more complex systems using whole proteoglycans.

To ensure reliable results from an interaction study, the immobilization strategy must not affect the interacting biomolecules. Two aspects of surface immobilization of GAGs were highlighted in this thesis project: i) the presence of introduced functional groups on the chain, and ii) the orientation of the GAG on the surface, controlled by the position of the surface attachment point. Functional groups introduced along the GAG chain were shown to influence subsequent interactions. To avoid this, and to better mimic the attachment of GAGs to a core protein, immobilization via the reducing end of the GAG by biotin-streptavidin binding was chosen as a preferred strategy for further interaction studies. Even though the end-on immobilization strategy has obvious benefits, the density of GAGs on the surface and the length of the GAG chains are two important aspects, where the optimal surface will depend on characteristics, e.g., size, of the interacting entity. A layer-by-layer assembly is another immobilization example were introduced functional groups are avoided, but where the GAG is complemented by the presence of a positively charged polymer.

The usefulness of the interaction platform was further assessed by studying the binding behavior of glycoprotein C, purified from herpes simplex virus type 1 (HSV-1). The presence of a highly glycosylated, mucin-like region, with a previously unclear function in binding, was shown to modulate the binding of the glycoprotein to the GAG. This likely has implications for the infectious mechanism of the virus, further suggested by cell studies, where attachment of virions having glycoproteins either with, or without this region, was compared. The binding of whole viruses to

end-on immobilized GAGs is currently being investigated using total internal reflection fluorescence (TIRF) microscopy, where the binding and unbinding of viruses are being probed in order to estimate kinetic parameters. In line with what has been presented herein, virions did not bind to non-sulfated HA but significantly to sulfated GAGs (**Figure 34**). To compare binding of different virus strains to GAGs using this setup can complement common cell-binding assays, and could potentially also be used to study the lateral movement of viruses on a surface.

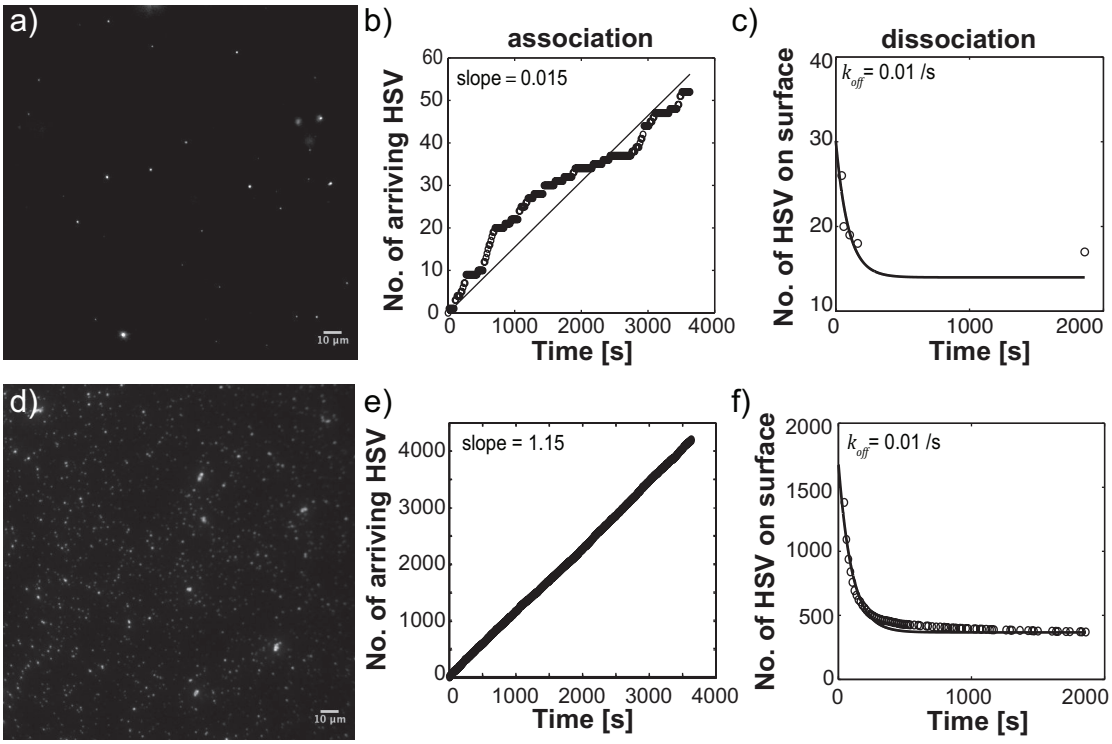

Figure 34. HSV-1 virions binding to a,b,c) b-HA and d,e,f) b-CS, immobilized to biotinylated SLBs (99% POPC + 1% DOPE-biotin). a, b) TIRF images showing fluorescently labeled HSV-1 virions bound to the surface. b,c,e,f) Counting the number of virus that bind and unbind can give information about kinetic characteristics. *Work in progress: Peerboom, Altgärde, Trybala, Bergström, Bally et al.*

The sulfation of GAGs is an aspect often discussed in literature as being a determinant in many binding events. In this thesis project, non-sulfated b-HA and two sulfated GAGs; the naturally sulfated b-CS and the synthetically sulfated b-sHA were used. For both virus glycoprotein and BMP-2, sulfation was a requisite for binding as very low binding was seen to b-HA in either case. Differences between b-CS and b-sHA was not as significant, indicating that either the need for specific patterns of sulfate groups are not pronounced for these proteins, or that the required GAG sequence is present in both the b-CS and the b-sHA used here. Further interaction studies, along with successful molecular sequencing and *de novo* synthesis of GAGs, are needed in order to find sequence-specific effects. This is also a prerequisite for the development of GAG-based drugs. As GAGs have a multitude of functions *in vivo*, isolation of the active sequence is needed to avoid cross-reactions and unwanted side effects. An

example of this is the anticoagulant drug heparin, which today is administered as a depolymerized variant or as a synthesized pentasaccharide.

In this thesis project, QCM-D and SPR were the main surface sensitive techniques. The benefits of using both of these techniques when measuring the formation of GAG layers are apparent when looking at the significant hydration of these molecules. The interface between immobilized hyaluronan and chondrocytes was studied using QCM-D in combination with light microscopy. The study suggested a degrading action of the cells on the underlying layer, and showed, more importantly, that the interface between cells and biomaterials can be studied using surface sensitive techniques even when cell attachment does not occur. To develop this approach further, growth factors, e.g., BMP-2 could be added to probe possible changes in the cell. Also, immobilized hyaluronan derivatives with a higher molecular weight, with and without *in situ* cross-linking, could better resemble scaffolds used in many *in vivo* applications.

Hopefully, this thesis project has emphasized the importance of GAGs in many biological mechanisms, and the kind of information that can be gained from studying them using surface-based analytical techniques. The use of such techniques to study GAG-based interactions is not new, but the immobilizing strategy and how it may influence the studied interaction is seldom regarded or discussed. The studies presented here highlight important factors to consider when designing GAG-presenting surfaces, to further unravel the functions and possibilities of GAGs *in vivo* and *in vitro*.

9
Acknowledgements

Although there is a single author of this thesis, many people have contributed either directly or indirectly to it. I'm so grateful for all the friends I have made during this time and although everyone has been important, some deserves a special recognition.

Sofia Svedhem, my supervisor, for most things! For all the time you spent answering questions and reading texts. And for your enthusiasm for science.

Fredrik Höök, my examiner, for support, encouragement and for an inspiring workplace.

Marta Bally, Angelika Kunze & Julie Gold, for advice and support whenever needed.

My co-authors & collaborators: Erik Nilebäck, Laura de Battice, Hanna Rydberg, the Biomedical Materials Group at Martin Luther University, INNOVENT, the FIND&BIND group, and clinical virology at Sahlgrenska. Without you, this would have been a very thin thesis.

The Biological Physics Group. I'm so happy to have shared my working days together with such curious, creative and caring group of people. Where else could you discuss such various topics as *how to date the Chinese wall* and *how to care for a stolen tucan*?

Hanna, my office-mate, for being an awesome thesis-writing coach; giving advice, hugs, pep-talks, chewing gums and most importantly great laughs!

Olof, for highlighting my mistakes (at least written ones) before print.

My family, for being the best! And for sometimes trying to figure out what I do.

Erik, for helping me through the tough times. For always supporting and never complaining. For tea and socks. I love you!

References

1 Gama, C. I.; Hsieh-Wilson, L. C., Chemical approaches to deciphering the glycosaminoglycan code. *Curr. Opin. Chem. Biol.* (2005) **9,** 609-619.

2 Raman, R.; Sasisekharan, V.; Sasisekharan, R., Structural Insights into biological roles of protein-glycosaminoglycan interactions. *Chem. Biol.* (2005) **12,** 267-277.

3 Hileman, R. E.; Fromm, J. R.; Weiler, J. M.; Linhardt, R. J., Glycosaminoglycan-protein interactions: Definition of consensus sites in glycosaminoglycan binding proteins. *BioEssays* (1998) **20,** 156-167.

4 Cooper, M. A., Label-free screening of bio-molecular interactions. *Anal. Bioanal. Chem.* (2003) **377,** 834-842.

5 Turner, A. P. F., Biosensors - Sense and sensitivity. *Science* (2000) **290,** 1315-1317.

6 Silbert, J. E.; Sugumaran, G., Biosynthesis of chondroitin/dermatan sulfate. *IUBMB Life* (2002) **54,** 177-186.

7 Laurent, T. C.; Fraser, J. R. E., Hyaluronan. *FASEB J.* (1992) **6,** 2397-2404.

8 Kusche-Gullberg, M.; Kjellén, L., Sulfotransferases in glycosaminoglycan biosynthesis. *Curr. Opin. Struct. Biol.* (2003) **13,** 605-611.

9 Toole, B. P., Hyaluronan: From extracellular glue to pericellular cue. *Nat. Rev. Cancer* (2004) **4,** 528-539.

10 Markovic´-Housley, Z.; Miglierini, G.; Soldatova, L.; Rizkallah, P. J.; Müller, U.; Schirmer, T., Crystal structure of hyaluronidase, a major allergen of bee venom. *Structure* (2000) **8,** 1025-1035.

11 Hopwood, J. J.; Robinson, H. C., The molecular weight distribution of glycosaminoglycans. *Biochem. J.* (1973) **135,** 631-637.

12 Sugahara, K.; Mikami, T.; Uyama, T.; Mizuguchi, S.; Nomura, K.; Kitagawa, H., Recent advances in the structural biology of chondroitin sulfate and dermatan sulfate. *Curr. Opin. Struct. Biol.* (2003) **13,** 612-620.

13 Schnabelrauch, M.; Scharnweber, D.; Schiller, J., Sulfated glycosaminoglycans as promising artificial extracellular matrix components to improve the regeneration of tissues. *Curr. Med. Chem.* (2013) **20,** 2501-2523.

14 Lamanna, W. C.; Kalus, I.; Padva, M.; Baldwin, R. J.; Merry, C. L. R.; Dierks, T., The heparanome-The enigma of encoding and decoding heparan sulfate sulfation. *J. Biotechnol.* (2007) **129,** 290-307.

15 Kitagawa, H.; Tsutsumi, K.; Tone, Y.; Sugahara, K., Developmental regulation of the sulfation profile of chondroitin sulfate chains in the chicken embryo brain. *J. Biol. Chem.* (1997) **272,** 31377-31381.

16 Uyama, T.; Ishida, M.; Izumikawa, T.; Trybala, E.; Tufaro, F.; Bergström, T.; Sugahara, K.; Kitagawa, H., Chondroitin 4-O-sulfotransferase-1 regulates E disaccharide expression of chondroitin sulfate required for herpes simplex virus infectivity. *J. Biol. Chem.* (2006) **281,** 38668-38674.

17 Sasisekharan, R.; Shriver, Z.; Venkataraman, G.; Narayanasami, U., Roles of heparan-sulphate glycosaminoglycans in cancer. *Nat. Rev. Cancer* (2002) **2,** 521-528.

18 Fernaud-Espinosa, I.; Nieto-Sampedro, M.; Bovolenta, P., Developmental distribution of glycosaminoglycans in embryonic rat brain: Relationship to axonal tract formation. *J. Neurobiol.* (1996) **30,** 410-424.
19 Dhoot, G. K.; Gustafsson, M. K.; Ai, X.; Sun, W.; Standiford, D. M.; Emerson C.P, Jr., Regulation of Wnt signaling and embryo patterning by an extracellular sulfatase. *Science* (2001) **293,** 1663-1666.
20 Khor, E.; Lim, L. Y., Implantable applications of chitin and chitosan. *Biomaterials* (2003) **24,** 2339-2349.
21 Mourya, V. K.; Inamdar, N. N., Chitosan-modifications and applications: Opportunities galore. *React. Funct. Polym.* (2008) **68,** 1013-1051.
22 Fischer, S.; Thümmler, K.; Volkert, B.; Hettrich, K.; Schmidt, I.; Fischer, K., Properties and applications of cellulose acetate. *Macromol. Symp.* (2008) **262,** 89-96.
23 Heinze, T.; Koschella, A., Carboxymethyl ethers of cellulose and starch - A review. *Macromol. Symp.* (2005) **223,** 13-39.
24 Xing, R.; Liu, S.; Yu, H.; Zhang, Q.; Li, Z.; Li, P., Preparation of low-molecular-weight and high-sulfate-content chitosans under microwave radiation and their potential antioxidant activity in vitro. *Carbohydr. Res.* (2004) **339,** 2515-2519.
25 Groth, T.; Wagenknecht, W., Anticoagulant potential of regioselective derivatized cellulose. *Biomaterials* (2001) **22,** 2719-2729.
26 Zhang, C.; Ping, Q.; Zhang, H.; Shen, J., Preparation of N-alkyl-O-sulfate chitosan derivatives and micellar solubilization of taxol. *Carbohydr. Polym.* (2003) **54,** 137-141.
27 Peschel, D.; Zhang, K.; Fischer, S.; Groth, T., Modulation of osteogenic activity of BMP-2 by cellulose and chitosan derivatives. *Acta Biomater.* (2012) **8,** 183-193.
28 Altgärde, N.; Nilebäck, E.; De Battice, L.; Pashkuleva, I.; Reis, R. L.; Becher, J.; Möller, S.; Schnabelrauch, M.; Svedhem, S., Probing the biofunctionality of biotinylated hyaluronan and chondroitin sulfate by hyaluronidase degradation and aggrecan interaction. *Acta Biomater.* (2013) **9,** 8158-8166.
29 Hintze, V.; Möller, S.; Schnabelrauch, M.; Bierbaum, S.; Viola, M.; Worch, H.; Scharnweber, D., Modifications of hyaluronan influence the interaction with human bone morphogenetic protein-4 (hBMP-4). *Biomacromolecules* (2009) **10,** 3290-3297.
30 Liu, H.; Zhang, Z.; Linhardt, R. J., Lessons learned from the contamination of heparin. *Nat. Prod. Rep.* (2009) **26,** 313-321.
31 Deangelis, P. L.; Liu, J.; Linhardt, R. J., Chemoenzymatic synthesis of glycosaminoglycans: Re-creating, re-modeling and re-designing nature's longest or most complex carbohydrate chains. *Glycobiology* (2013) **23,** 764-777.
32 Orgueira, H. A.; Bartolozzi, A.; Schell, P.; Litjens, R. E. J. N.; Palmacci, E. R.; Seeberger, P. H., Modular synthesis of heparin oligosaccharides. *Chemistry - A European Journal* (2003) **9,** 140-169.
33 Furie, B.; Furie, B. C., The molecular basis of blood coagulation. *Cell* (1988) **53,** 505-518.
34 Bourin, M.; Lindahl, U., Glycosaminoglycans and the regulation of blood coagulation. *Biochem. J.* (1993) **289,** 313-330.

35 Petitou, M.; Casu, B.; Lindahl, U., 1976-1983, a critical period in the history of heparin: The discovery of the antithrombin binding site. *Biochimie* (2003) **85,** 83-89.
36 Seeberger, P. H.; Werz, D. B., Synthesis and medical applications of oligosaccharides. *Nature* (2007) **446,** 1046-1051.
37 Tollefsen, D. M.; Pestka, C. A.; Monafo, W. J., Activation of heparin cofactor II by dermatan sulfate. *J. Biol. Chem.* (1983) **258,** 6713-6716.
38 Scully, M. F.; Ellis, V.; Seno, N.; Kakkar, V. V., Effect of oversulphated chondroitin and dermatan sulphate upon thrombin and factor Xa inactivation by antithrombin III or heparin cofactor II. *Biochem. J.* (1988) **254,** 547-551.
39 Barbucci, R.; Magnani, A.; Lamponi, S.; Albanese, A., Chemistry and biology of glycosaminoglycans in blood coagulation. *Polym. Adv. Technol.* (1996) **7,** 675-685.
40 Verheye, S.; Markou, C. P.; Salame, M. Y.; Wan, B.; King III, S. B.; Robinson, K. A.; Chronos, N. A. F.; Hanson, S. R., Reduced thrombus formation by hyaluronic acid coating of endovascular devices. *Arterioscler., Thromb., Vasc. Biol.* (2000) **20,** 1168-1172.
41 Volný, M.; Elam, W. T.; Ratner, B. D.; Tureček, F., Enhanced in-vitro blood compatibility of 316L stainless steel surfaces by reactive landing of hyaluronan ions. *J. Biomed. Mater. Res., Part B* (2007) **80,** 505-510.
42 Thierry, B.; Winnik, F. M.; Merhi, Y.; Griesser, H. J.; Tabrizian, M., Biomimetic hemocompatible coatings through immobilization of hyaluronan derivatives on metal surfaces. *Langmuir* (2008) **24,** 11834-11841.
43 Harker, L. A., Role of platelets and thrombosis in mechanisms of acute occlusion and restenosis after angioplasty. *Am. J. Cardiol.* (1987) **60,** 20B-28B.
44 Buckwalter, J. A.; Rosenberg, L. C., Electron microscopic studies of cartilage proteoglycans. Direct evidence for the variable length of the chondroitin sulfate-rich region of proteoglycan subunit core protein. *J. Biol. Chem.* (1982) **257,** 9830-9839.
45 Knudson, C. B.; Knudson, W., Hyaluronan-binding proteins in development, tissue homeostasis, and disease. *FASEB J.* (1993) **7,** 1233-1241.
46 Heng, B. C.; Gribbon, P. M.; Day, A. J.; Hardingham, T. E., Hyaluronan binding to Link module of TSG-6 and to G1 domain of aggrecan is differently regulated by pH. *J. Biol. Chem.* (2008) **283,** 32294-32301.
47 Scott, J. E., Proteoglycan-fibrillar collagen interactions. *Biochem. J.* (1988) **252,** 313-323.
48 Douglas, T.; Heinemann, S.; Mietrach, C.; Hempel, U.; Bierbaum, S.; Scharnweber, D.; Worch, H., Interactions of collagen types I and II with chondroitin sulfates A-C and their effect on osteoblast adhesion. *Biomacromolecules* (2007) **8,** 1085-1092.
49 Seror, J.; Merkher, Y.; Kampf, N.; Collinson, L.; Day, A. J.; Maroudas, A.; Klein, J., Articular cartilage proteoglycans as boundary lubricants: Structure and frictional interaction of surface-attached hyaluronan and hyaluronan-aggrecan complexes. *Biomacromolecules* (2011) **12,** 3432-3443.
50 Baranova, N. S.; Attili, S.; Wolny, P. M.; Richter, R. P., The sweet coat of living cells - From supramolecular structure and dynamics to biological function. *Int. J. Mater. Res.* (2011) **102,** 903-905.

51 Bastow, E. R.; Byers, S.; Golub, S. B.; Clarkin, C. E.; Pitsillides, A. A.; Fosang, A. J., Hyaluronan synthesis and degradation in cartilage and bone. *Cell. Mol. Life Sci.* (2008) **65,** 395-413.

52 Salustri, A.; Garlanda, C.; Hirsch, E.; De Acetis, M.; Maccagno, A.; Bottazi, B.; Doni, A.; Bastone, A.; Mantovani, G.; Peccoz, P. B.; Salvatori, G.; Mahoney, D. J.; Day, A. J.; Siracusa, G.; Romani, L.; Mantovani, A., PTX3 plays a key role in the organization of the cumulus oophorus extracellular matrix and in in vivo fertilization. *Development* (2004) **131,** 1577-1586.

53 Smorenburg, S. M.; Van Noorden, C. J. F., The complex effects of heparins on cancer progression and metastasis in experimental studies. *Pharmacol. Rev.* (2001) **53,** 93-105.

54 Ruoslahti, E.; Yamaguchi, Y., Proteoglycans as modulators of growth factor activities. *Cell* (1991) **64,** 867-869.

55 Wang, E. A.; Rosen, V.; D'Alessandro, J. S.; Bauduy, M.; Cordes, P.; Harada, T.; Israel, D. I.; Hewick, R. M.; Kerns, K. M.; Lapan, P.; Luxenberg, D. P.; McQuaid, D.; Moutsatsos, I. K.; Nove, J.; Wozney, J. M., Recombinant human bone morphogenetic protein induces bone formation. *Proc. Natl. Acad. Sci. U. S. A.* (1990) **87,** 2220-2224.

56 Katagiri, T.; Yamaguchi, A.; Komaki, M.; Abe, E.; Takahashi, N.; Ikeda, T.; Rosen, V.; Wozney, J. M.; Fujisawa-Sehara, A.; Suda, T., Bone morphogenetic protein-2 converts the differentiation pathway of C2C12 myoblasts into the osteoblast lineage. *J. Cell Biol.* (1994) **127,** 1755-1766.

57 Zhao, B.; Katagiri, T.; Toyoda, H.; Takada, T.; Yanai, T.; Fukuda, T.; Chung, U. I.; Koike, T.; Takaoka, K.; Kamijo, R., Heparin potentiates the in Vivo ectopic bone formation induced by bone morphogenetic protein-2. *J. Biol. Chem.* (2006) **281,** 23246-23253.

58 Salbach, J.; Rachner, T. D.; Rauner, M.; Hempel, U.; Anderegg, U.; Franz, S.; Simon, J. C.; Hofbauer, L. C., Regenerative potential of glycosaminoglycans for skin and bone. *J. Mol. Med.* (2012) **90,** 625-635.

59 Wollenweber, M.; Domaschke, H.; Hanke, T.; Boxberger, S.; Schmack, G.; Gliesche, K.; Scharnweber, D.; Worch, H., Mimicked bioartificial matrix containing chondroitin sulphate on a textile scaffold of poly(3-hydroxybutyrate) alters the differentiation of adult human mesenchymal stem cells. *Tissue Eng.* (2006) **12,** 345-359.

60 Campoccia, D.; Doherty, P.; Radice, M.; Brun, P.; Abatangelo, G.; Williams, D. F., Semisynthetic resorbable materials from hyaluronan esterification. *Biomaterials* (1998) **19,** 2101-2127.

61 Dehne, T.; Karlsson, C.; Ringe, J.; Sittinger, M.; Lindahl, A., Chondrogenic differentiation potential of osteoarthritic chondrocytes and their possible use in matrix-associated autologous chondrocyte transplantation. *Arthritis Res. Ther.* (2009) **11**.

62 Shu, X. Z.; Liu, Y.; Palumbo, F. S.; Luo, Y.; Prestwich, G. D., In situ crosslinkable hyaluronan hydrogels for tissue engineering. *Biomaterials* (2004) **25,** 1339-1348.

63 Picart, C., Polyelectrolyte multilayer film: From physico-chemical properties to the control of cellular processes. *Curr. Med. Chem.* (2008) **15,** 685-697.

64 Crouzier, T.; Picart, C., Ion pairing and hydration in polyelectrolyte multilayer films containing polysaccharides. *Biomacromolecules* (2009) **10,** 433-442.

65 Macdonald, M. L.; Samuel, R. E.; Shah, N. J.; Padera, R. F.; Beben, Y. M.; Hammond, P. T., Tissue integration of growth factor-eluting layer-by-layer polyelectrolyte multilayer coated implants. *Biomaterials* (2011) **32,** 1446-1453.
66 Almodóvar, J.; Bacon, S.; Gogolski, J.; Kisiday, J. D.; Kipper, M. J., Polysaccharide-based polyelectrolyte multilayer surface coatings can enhance mesenchymal stem cell response to adsorbed growth factors. *Biomacromolecules* (2010) **11,** 2629-2639.
67 Crouzier, T.; Ren, K.; Nicolas, C.; Roy, C.; Picart, C., Layer-by-layer films as a biomimetic reservoir for rhBMP-2 delivery: Controlled differentiation of myoblasts to osteoblasts. *Small* (2009) **5,** 598-608.
68 Bergman, K.; Engstrand, T.; Hilborn, J.; Ossipov, D.; Piskounova, S.; Bowden, T., Injectable cell-free template for bone-tissue formation. *J. Biomed. Mater. Res., Part A* (2009) **91,** 1111-1118.
69 Vaheri, A., Heparin and related polyionic substances as virus inhibitors. *Acta Pathol. Microbiol. Scand. Suppl.* (1964) SUPPL 171:1-98.
70 WuDunn, D.; Spear, P. G., Initial interaction of herpes simplex virus with cells is binding to heparan sulfate. *J. Virol.* (1989) **63,** 52-58.
71 Krusat, T.; Streckert, H. J., Heparin-dependent attachment of respiratory syncytial virus (RSV) to host cells. *Arch. Virol.* (1997) **142,** 1247-1254.
72 Salvador, B.; Sexton, N. R.; Carrion, R.; Nunneley, J.; Patterson, J. L.; Steffen, I.; Lu, K.; Muench, M. O.; Lembo, D.; Simmons, G., Filoviruses utilize glycosaminoglycans for their attachment to target cells. *J. Virol.* (2013) **87,** 3295-3304.
73 Saphire, A. C. S.; Bobardt, M. D.; Zhang, Z.; David, G.; Gallay, P. A., Syndecans serve as attachment receptors for human immunodeficiency virus type 1 on macrophages. *J. Virol.* (2001) **75,** 9187-9200.
74 Trybala, E.; Liljeqvist, J. A.; Svennerholm, B.; Bergström, T., Herpes simplex virus types 1 and 2 differ in their interaction with heparan sulfate. *J. Virol.* (2000) **74,** 9106-9114.
75 Mårdberg, K.; Trybala, E.; Tufaro, F.; Bergström, T., Herpes simplex virus type 1 glycoprotein C is necessary for efficient infection of chondroitin sulfate-expressing gro2C cells. *J. Gen. Virol.* (2002) **83,** 291-300.
76 Mårdberg, K.; Trybala, E.; Glorioso, J. C.; Bergström, T., Mutational analysis of the major heparan sulfate-binding domain of herpes simplex virus type 1 glycoprotein C. *J. Gen. Virol.* (2001) **82,** 1941-1950.
77 Tal-Singer, R.; Peng, C.; Ponce de Leon, M.; Abrams, W. R.; Banfield, B. W.; Tufaro, F.; Cohen, G. H.; Eisenberg, R. J., Interaction of herpes simplex virus glycoprotein gC with mammalian cell surface molecules. *J. Virol.* (1995) **69,** 4471-4483.
78 Trybala, E.; Bergstrom, T.; Svennerholm, B.; Jeansson, S.; Glorioso, J. C.; Olofsson, S., Localization of a functional site on herpes simplex virus type 1 glycoprotein C involved in binding to cell surface heparan sulphate. *J. Gen. Virol.* (1994) **75,** 743-752.
79 Wadström, T.; Ljungh, Å., Glycosaminoglycan-binding microbial proteins in tissue adhesion and invasion: Key events in microbial pathogenicity. *J. Med. Microbiol.* (1999) **48,** 223-233.
80 Spillmann, D., Heparan sulfate: Anchor for viral intruders? *Biochimie* (2001) **83,** 811-817.

81 Su, C. M.; Liao, C. L.; Lee, Y. L.; Lin, Y. L., Highly sulfated forms of heparin sulfate are involved in Japanese encephalitis virus infection. *Virology* (2001) **286,** 206-215.
82 Martinez, I.; Melero, J. A., Binding of human respiratory syncytial virus to cells: Implication of sulfated cell surface proteoglycans. *J. Gen. Virol.* (2000) **81,** 2715-2722.
83 Rider, C. C., The potential for heparin and its derivatives in the therapy and prevention of HIV-1 infection. *Glycoconjugate J.* (1997) **14,** 639-642.
84 Cooke, B. M.; Rogerson, S. J.; Brown, G. V.; Coppel, R. L., Adhesion of malaria-infected red blood cells to chondroitin sulfate A under flow conditions. *Blood* (1996) **88,** 4040-4044.
85 Ekblad, M.; Adamiak, B.; Bergefall, K.; Nenonen, H.; Roth, A.; Bergstrom, T.; Ferro, V.; Trybala, E., Molecular basis for resistance of herpes simplex virus type 1 mutants to the sulfated oligosaccharide inhibitor PI-88. *Virology* (2007) **367,** 244-252.
86 Mathias, D. K.; Pastrana-Mena, R.; Ranucci, E.; Tao, D.; Ferruti, P.; Ortega, C.; Staples, G. O.; Zaia, J.; Takashima, E.; Tsuboi, T.; Borg, N. A.; Verotta, L.; Dinglasan, R. R., A Small Molecule Glycosaminoglycan Mimetic Blocks Plasmodium Invasion of the Mosquito Midgut. *PLoS Pathog.* (2013) **9**.
87 Nyberg, K.; Ekblad, M.; Bergström, T.; Freeman, C.; Parish, C. R.; Ferro, V.; Trybala, E., The low molecular weight heparan sulfate-mimetic, PI-88, inhibits cell-to-cell spread of herpes simplex virus. *Antiviral Res.* (2004) **63,** 15-24.
88 Park, S.; Gildersleeve, J. C.; Blixt, O.; Shin, I., Carbohydrate microarrays. *Chem. Soc. Rev.* (2013) **42,** 4310-4326.
89 Jelinek, R.; Kolusheva, S., Carbohydrate biosensors. *Chem. Rev.* (2004) **104,** 5987-6015.
90 Gemma, E.; Meyer, O.; Uhrín, D.; Hulme, A. N., Enabling methodology for the end functionalisation of glycosaminoglycan oligosaccharides. *Mol. BioSyst.* (2008) **4,** 481-495.
91 Sackmann, E., Supported membranes: Scientific and practical applications. *Science* (1996) **271,** 43-48.
92 Richter, R. P.; Bérat, R.; Brisson, A. R., Formation of solid-supported lipid bilayers: An integrated view. *Langmuir* (2006) **22,** 3497-3505.
93 Zasadzinski, J. A.; Viswanthan, R.; Madsen, L.; Garnaes, J.; Schwartz, D. K., Langmuir-Blodgett Films. *Science* (1994) **263,** 1726-1733.
94 Keller, C. A.; Kasemo, B., Surface specific kinetics of lipid vesicle adsorption measured with a quartz crystal microbalance. *Biophys. J.* (1998) **75,** 1397-1402.
95 Reviakine, I.; Brisson, A., Formation of supported phospholipid bilayers from unilamellar vesicles investigated by atomic force microscopy. *Langmuir* (2000) **16,** 1806-1815.
96 Cho, N. J.; Frank, C. W., Fabrication of a planar zwitterionic lipid bilayer on titanium oxide. *Langmuir* (2010) **26,** 15706-15710.
97 Boudard, S.; Seantier, B.; Breffa, C.; Decher, G.; Félix, O., Controlling the pathway of formation of supported lipid bilayers of DMPC by varying the sodium chloride concentration. *Thin Solid Films* (2006) **495,** 246-251.
98 Rossetti, F. F.; Textor, M.; Reviakine, I., Asymmetric distribution of phosphatidyl serine in supported phospholipid bilayers on titanium dioxide. *Langmuir* (2006) **22,** 3467-3473.

99 Svedhem, S.; Dahlborg, D.; Ekeroth, J.; Kelly, J.; Höök, F.; Gold, J., In situ peptide-modified supported lipid bilayers for controlled cell attachment. *Langmuir* (2003) **19,** 6730-6736.
100 Larsson, C.; Rodahl, M.; Höök, F., Characterization of DNA immobilization and subsequent hybridization on a 2D arrangement of streptavidin on a biotin-modified lipid bilayer supported on SiO2. *Anal. Chem.* (2003) **75,** 5080-5087.
101 Richter, R. P.; Him, J. L. K.; Tessier, B.; Tessier, C.; Brisson, A. R., On the kinetics of adsorption and two-dimensional self-assembly of annexin A5 on supported lipid bilayers. *Biophys. J.* (2005) **89,** 3372-3385.
102 Ulman, A., Formation and structure of self-assembled monolayers. *Chem. Rev.* (1996) **96,** 1533-1554.
103 Sigal, G. B.; Bamdad, C.; Barberis, A.; Strominger, J.; Whitesides, G. M., A self-assembled monolayer for the binding and study of histidine-tagged proteins by surface plasmon resonance. *Anal. Chem.* (1996) **68,** 490-497.
104 Prime, K. L.; Whitesides, G. M., Adsorption of proteins onto surfaces containing end-attached oligo(ethylene oxide): A model system using self-assembled monolayers. *J. Am. Chem. Soc.* (1993) **115,** 10714-10721.
105 Nilebäck, E.; Feuz, L.; Uddenberg, H.; Valiokas, R.; Svedhem, S., Characterization and application of a surface modification designed for QCM-D studies of biotinylated biomolecules. *Biosens. Bioelectron.* (2011) **28,** 407-413.
106 Johnsson, B.; Löfås, S.; Lindquist, G., Immobilization of proteins to a carboxymethyldextran-modified gold surface for biospecific interaction analysis in surface plasmon resonance sensors. *Anal. Biochem.* (1991) **198,** 268-277.
107 Anjaneyulu, P. S.; Staros, J. V., Reactions of N-hydroxysulfosuccinimide active esters. *Int. J. Pept. Protein Res.* (1987) **30,** 117-124.
108 Uygun, B. E.; Stojsih, S. E.; Matthew, H. W. T., Effects of immobilized glycosaminoglycans on the proliferation and differentiation of mesenchymal stem cells. *Tissue Eng. - Part A* (2009) **15,** 3499-3512.
109 Popplewell, J. F.; Swann, M. J.; Ahmed, Y.; Turnbull, J. E.; Fernig, D. G., Fabrication of carbohydrate surfaces by using nonderivatised oligosaccharides, and their application to measuring the assembly of sugar-protein complexes. *ChemBioChem* (2009) **10,** 1218-1226.
110 Hoffman, J.; Larm, O.; Scholander, E., A new method for covalent coupling of heparin and other glycosaminoglycans to substances containing primary amino groups. *Carbohydr. Res.* (1983) **117,** 328-331.
111 Wang, K.; Luo, Y., Defined surface immobilization of glycosaminoglycan molecules for probing and modulation of cell-material interactions. *Biomacromolecules* (2013) **14,** 2373-2382.
112 Köwitsch, A.; Jurado Abreu, M.; Chhalotre, A.; Hielscher, M.; Fischer, S.; Mäder, K.; Groth, T., Synthesis of thiolated glycosaminoglycans and grafting to solid surfaces. *Carbohydr. Polym.* (2014) **114,** 344-351.
113 DeFife, K. M.; Shive, M. S.; Hagen, K. M.; Clapper, D. L.; Anderson, J. M., Effects of photochemically immobilized polymer coatings on protein adsorption, cell adhesion, and the foreign body reaction to silicone rubber. *J. Biomed. Mater. Res.* (1999) **44,** 298-307.
114 Wilchek, M.; Bayer, E. A., The avidin-biotin complex in bioanalytical applications. *Anal. Biochem.* (1988) **171,** 1-32.

115 Chaiet, L.; Wolf, F. J., The properties of streptavidin, a biotin-binding protein produced by Streptomycetes. *Arch. Biochem. Biophys.* (1964) **106,** 1-5.
116 Vermette, P.; Gengenbach, T.; Divisekera, U.; Kambouris, P. A.; Griesser, H. J.; Meagher, L., Immobilization and surface characterization of NeutrAvidin biotin-binding protein on different hydrogel interlayers. *J. Colloid Interface Sci.* (2003) **259,** 13-26.
117 Lee, J. W.; Sim, S. J.; Cho, S. M.; Lee, J., Characterization of a self-assembled monolayer of thiol on a gold surface and the fabrication of a biosensor chip based on surface plasmon resonance for detecting anti-GAD antibody. *Biosens. Bioelectron.* (2005) **20,** 1422-1427.
118 Richter, R. P.; Hock, K. K.; Burkhartsmeyer, J.; Boehm, H.; Bingen, P.; Wang, G.; Steinmetz, N. F.; Evans, D. J.; Spatz, J. P., Membrane-grafted hyaluronan films: A well-defined model system of glycoconjugate cell coats. *J. Am. Chem. Soc.* (2007) **129,** 5306-5307.
119 Rux, A. H.; Lou, H.; Lambris, J. D.; Friedman, H. M.; Eisenberg, R. J.; Cohen, G. H., Kinetic analysis of glycoprotein C of herpes simplex virus types 1 and 2 binding to heparin, heparan sulfate, and complement component C3b. *Virology* (2002) **294,** 324-332.
120 Mach, H.; Volkin, D. B.; Burke, C. J.; Russell Middaugh, C.; Linhardt, R. J.; Fromm, J. R.; Loganathan, D.; Mattsson, L., Nature of the interaction of heparin with acidic fibroblast growth factor. *Biochemistry* (1993) **32,** 5480-5489.
121 Osmond, R. I. W.; Kett, W. C.; Skett, S. E.; Coombe, D. R., Protein-heparin interactions measured by BIAcore 2000 are affected by the method of heparin immobilization. *Anal. Biochem.* (2002) **310,** 199-207.
122 Baranova, N. S.; Nilebäck, E.; Haller, F. M.; Briggs, D. C.; Svedhem, S.; Day, A. J.; Richter, R. P., The inflammation-associated protein TSG-6 cross-links hyaluronan via hyaluronan-induced TSG-6 oligomers. *J. Biol. Chem.* (2011) **286,** 25675-25686.
123 Alban, S.; Gastpar, R., Development of SPC-ELISA: A new assay principle for the study of sulfated polysaccharide-protein interactions. *J. Biomol. Screen.* (2001) **6,** 393-400.
124 Shipp, E. L.; Hsieh-Wilson, L. C., Profiling the Sulfation Specificities of Glycosaminoglycan Interactions with Growth Factors and Chemotactic Proteins Using Microarrays. *Chem. Biol.* (2007) **14,** 195-208.
125 Decher, G.; Hong, J. D.; Schmitt, J., Buildup of ultrathin multilayer films by a self-assembly process: III. Consecutively alternating adsorption of anionic and cationic polyelectrolytes on charged surfaces. *Thin Solid Films* (1992) **210–211, Part 2,** 831-835.
126 McAloney, R. A.; Sinyor, M.; Dudnik, V.; Cynthia Goh, M., Atomic force microscopy studies of salt effects on polyelectrolyte multilayer film morphology. *Langmuir* (2001) **17,** 6655-6663.
127 Yoo, D.; Shiratori, S. S.; Rubner, M. F., Controlling bilayer composition and surface wettability of sequentially adsorbed multilayers of weak polyelectrolytes. *Macromolecules* (1998) **31,** 4309-4318.
128 Engler, A. J.; Richert, L.; Wong, J. Y.; Picart, C.; Discher, D. E., Surface probe measurements of the elasticity of sectioned tissue, thin gels and polyelectrolyte multilayer films: Correlations between substrate stiffness and cell adhesion. *Surf. Sci.* (2004) **570,** 142-154.

129 Picart, C.; Mutterer, J.; Richert, L.; Luo, Y.; Prestwich, G. D.; Schaaf, P.; Voegel, J. C.; Lavalle, P., Molecular basis for the explanation of the exponential growth of polyelectrolyte multilayers. *Proc. Natl. Acad. Sci. U. S. A.* (2002) **99,** 12531-12535.
130 Lavalle, P.; Picart, C.; Mutterer, J.; Gergely, C.; Reiss, H.; Voegel, J. C.; Senger, B.; Schaaf, P., Modeling the Buildup of Polyelectrolyte Multilayer Films Having Exponential Growth. *J. Phys. Chem. B* (2004) **108,** 635-648.
131 Gong, Y.; Zhu, Y.; Liu, Y.; Ma, Z.; Gao, C.; Shen, J., Layer-by-layer assembly of chondroitin sulfate and collagen on aminolyzed poly(l-lactic acid) porous scaffolds to enhance their chondrogenesis. *Acta Biomater.* (2007) **3,** 677-685.
132 Kirchhof, K.; Andar, A.; Yin, H. B.; Gadegaard, N.; Riehle, M. O.; Groth, T., Polyelectrolyte multilayers generated in a microfluidic device with pH gradients direct adhesion and movement of cells. *Lab Chip* (2011) **11,** 3326-3335.
133 Richert, L.; Lavalle, P.; Vautier, D.; Senger, B.; Stoltz, J. F.; Schaaf, P.; Voegel, J. C.; Picart, C., Cell interactions with polyelectrolyte multilayer films. *Biomacromolecules* (2002) **3,** 1170-1178.
134 Decher, G., Fuzzy nanoassemblies: Toward layered polymeric multicomposites. *Science* (1997) **277,** 1232-1237.
135 Spillmann, D.; Lindahl, U., Glycosaminoglycan-protein interactions: A question of specificity. *Curr. Opin. Struct. Biol.* (1994) **4,** 677-682.
136 Israelachvili, J., *Intermolecular and surface forces*. 2nd ed.; Academic Press: 1991.
137 Ball, V.; Maechling, C., Isothermal microcalorimetry to investigate non specific interactions in biophysical chemistry. *Int. J. Mol. Sci.* (2009) **10,** 3283-3315.
138 Margalit, H.; Fischer, N.; Ben-Sasson, S. A., Comparative analysis of structurally defined heparin binding sequences reveals a distinct spatial distribution of basic residues. *J. Biol. Chem.* (1993) **268,** 19228-19231.
139 Rodriguez-Carvajal, M. A.; Imberty, A.; Pérez, S., Conformational behavior of chondroitin and chondroitin sulfate in relation to their physical properties as inferred by molecular modeling. *Biopolymers* (2003) **69,** 15-28.
140 Scott, J. E., Supramolecular organization of extracellular matrix glycosaminoglycans, in vitro and in the tissues. *FASEB J.* (1992) **6,** 2639-2645.
141 Scott, J. E.; Heatley, F., Biological properties of hyaluronan in aqueous solution are controlled and sequestered by reversible tertiary structures, defined by NMR spectroscopy. *Biomacromolecules* (2002) **3,** 547-553.
142 Raman, R.; Venkataraman, G.; Ernst, S.; Sasisekharan, V.; Sasisekharan, R., Structural specificity of heparin binding in the fibroblast growth factor family of proteins. *Proc. Natl. Acad. Sci. U. S. A.* (2003) **100,** 2357-2362.
143 Kiessling, L. L.; Young, T.; Gruber, T. D.; Mortell, K. H., Multivalency in Protein–Carbohydrate Recognition. In *Glycoscience*, Springer-Verlag Berlin Heidelberg: 2008.
144 Mammen, M.; Choi, S. K.; Whitesides, G. M., Polyvalent interactions in biological systems: Implications for design and use of multivalent ligands and inhibitors. *Angew. Chem., Int. Ed.* (1998) **37,** 2755-2794.
145 Zhang, Y.; Luo, S.; Tang, Y.; Yu, L.; Hou, K. Y.; Cheng, J. P.; Zeng, X.; Wang, P. G., Carbohydrate-protein interactions by "clicked" carbohydrate self-assembled monolayers. *Anal. Chem.* (2006) **78,** 2001-2008.

146 Hill, A. V., The Combinations of Haemoglobin with Oxygen and with Carbon Monoxide. I. *Biochem. J.* (1913) **7,** 471-80.
147 Weiss, J. N., The Hill equation revisited: Uses and misuses. *FASEB J.* (1997) **11,** 835-841.
148 Ward, M. D.; Buttry, D. A., In situ interfacial mass detection with piezoelectric transducers. *Science* (1990) **249,** 1000-1007.
149 Cady, W. G., The piezoelectric resonator. *Phys. Rev. A* (1921) **17,** 531-533.
150 Sauerbrey, G. Z., Verwendung von Schwingquarzen zur Wägung dünner Schichten und zur Mikrowägung. *Z. Phys. A: Hadrons Nucl.* (1959) **155,** 206-222.
151 Keiji Kanazawa, K.; Gordon Ii, J. G., Frequency of a quartz microbalance in contact with liquid. *Anal. Chem.* (1985) **57,** 1770-1771.
152 Reimhult, E.; Larsson, C.; Kasemo, B.; Höök, F., Simultaneous surface plasmon resonance and quartz crystal microbalance with dissipation monitoring measurements of biomolecular adsorption events involving structural transformations and variations in coupled water. *Anal. Chem.* (2004) **76,** 7211-7220.
153 Reviakine, I.; Johannsmann, D.; Richter, R. P., Hearing what you cannot see and visualizing what you hear: Interpreting quartz crystal microbalance data from solvated interfaces. *Anal. Chem.* (2011) **83,** 8838-8848.
154 Reviakine, I. D., Johannsmann, D., Richter, R. P., Hearing what you can't see and visualizing what you hear: interpreting quartz crystal microbalance data from solvated interfaces. *Analytical Chemistry, just accepted* (2011).
155 Voinova, M. V.; Jonson, M.; Kasemo, B., 'Missing mass' effect in biosensor's QCM applications. *Biosens. Bioelectron.* (2002) **17,** 835-841.
156 Voinova, M. V.; Rodahl, M.; Jonson, M.; Kasemo, B., Viscoelastic acoustic response of layered polymer films at fluid-solid interfaces: Continuum mechanics approach. *Phys. Scr.* (1999) **59,** 391-396.
157 Liedberg, B.; Lundström, I.; Stenberg, E., Principles of biosensing with an extended coupling matrix and surface plasmon resonance. *Sens. Actuators, B* (1993) **11,** 63-72.
158 Liedberg, B.; Nylander, C.; Lunström, I., Surface plasmon resonance for gas detection and biosensing. *Sensors and Actuators* (1983) **4,** 299-304.
159 Kretschmann, E., The determination of the optical constants of metals by excitation of surface plasmons. *Eur. Phys. J. A* (1971) **241,** 313-324.
160 Nico J. De Mol, M. J. E. F., *Surface Plasmon Resonance: Methods and Protocolls*. Springer protocols: 2010; Vol. 627.
161 Löfås, S.; Malmqvist, M.; Rönnberg, I.; Stenberg, E.; Liedberg, B.; Lundström, I., Bioanalysis with surface plasmon resonance. *Sens. Actuators, B* (1991) **5,** 79-84.
162 Axelrod, D.; Koppel, D. E.; Schlessinger, J.; Elson, E.; Webb, W. W., Mobility measurement by analysis of fluorescence photobleaching recovery kinetics. *Biophys. J.* (1976) **16,** 1055-1069.
163 Meyvis, T. K. L.; De Smedt, S. C.; Van Oostveldt, P.; Demeester, J., Fluorescence recovery after photobleaching: A versatile tool for mobility and interaction measurements in pharmaceutical research. *Pharm. Res.* (1999) **16,** 1153-1162.
164 Jönsson, P.; Jonsson, M. P.; Tegenfeldt, J. O.; Höök, F., A method improving the accuracy of fluorescence recovery after photobleaching analysis. *Biophys. J.* (2008) **95,** 5334-5348.

165 Stern, O., Zur Theorie der Elektrolytischen Doppelschicht. *Z. Elektrochem* (1924) **30,** 508-516.
166 Werner, C.; Körber, H.; Zimmermann, R.; Dukhin, S.; Jacobasch, H.-J., Extended Electrokinetic Characterization of Flat Solid Surfaces. *J. Colloid Interface Sci.* (1998) **208,** 329-346.
167 Menzies, K. L.; Jones, L., The impact of contact angle on the biocompatibility of biomaterials. *Optometry Vision Sci.* (2010) **87,** 387-399.
168 Cassie, A. B. D., Contact angles. *Discussions of the Faraday Society* (1948) **3,** 11-16.
169 Young, T., An Essay on the Cohesion of Fluids. *Philosophical Transactions of the Royal Society of London* (1805) **95,** 65-87.
170 Tavana, H.; Neumann, A. W., Recent progress in the determination of solid surface tensions from contact angles. *Adv. Colloid Interface Sci.* (2007) **132,** 1-32.
171 Zisman, W. A., Advances in chemistry. *American Chemical Society* (1964) **43,** 1.
172 Glasmästar, K.; Larsson, C.; Höök, F.; Kasemo, B., Protein adsorption on supported phospholipid bilayers. *J. Colloid Interface Sci.* (2002) **246,** 40-47.
173 Hokputsa, S.; Jumel, K.; Alexander, C.; Harding, S. E., Hydrodynamic characterisation of chemically degraded hyaluronic acid. *Carbohydr. Polym.* (2003) **52,** 111-117.
174 Horkay, F.; Basser, P. J.; Hecht, A. M.; Geissler, E., Chondroitin sulfate in solution: Effects of mono- and divalent salts. *Macromolecules* (2012) **45,** 2882-2890.
175 DeAngelis, P. L.; Gunay, N. S.; Toida, T.; Mao, W. J.; Linhardt, R. J., Identification of the capsular polysaccharides of Type D and F Pasteurella multocida as unmodified heparin and chondroitin, respectively. *Carbohydr. Res.* (2002) **337,** 1547-1552.
176 Satoh, A.; Toida, T.; Yoshida, K.; Kojima, K.; Matsumoto, I., New role of glycosaminoglycans on the plasma membrane proposed by their interaction with phosphatidylcholine. *FEBS Lett.* (2000) **477,** 249-252.
177 Micciulla, S.; Dodoo, S.; Chevigny, C.; Laschewsky, A.; Von Klitzing, R., Short versus long chain polyelectrolyte multilayers: A direct comparison of self-assembly and structural properties. *Phys. Chem. Chem. Phys.* (2014) **16,** 21988-21998.
178 Ruppert, R.; Hoffmann, E.; Sebald, W., Human bone morphogenetic protein 2 contains a heparin-binding site which modifies its biological activity. *Eur. J. Biochem.* (1996) **237,** 295-302.
179 Laub, M.; Seul, T.; Schmachtenberg, E.; Jennissen, H. P., Molecular modelling of bone morphogenetic protein-2 (BMP-2) by 3D-rapid prototyping. *Materialwiss. Werkst.* (2001) **32,** 926-930.
180 Stern, R.; Kogan, G.; Jedrzejas, M. J.; Šoltés, L., The many ways to cleave hyaluronan. *Biotech. Adv.* (2007) **25,** 537-557.
181 Girish, K. S.; Kemparaju, K., The magic glue hyaluronan and its eraser hyaluronidase: A biological overview. *Life Sci.* (2007) **80,** 1921-1943.
182 El-Safory, N. S.; Fazary, A. E.; Lee, C. K., Hyaluronidases, a group of glycosidases: Current and future perspectives. *Carbohydr. Polym.* (2010) **81,** 165-181.
183 Hardingham, T. E.; Fosang, A. J., Proteoglycans: Many forms and many functions. *FASEB J.* (1992) **6,** 861-870.

184 Ng, L.; Grodzinsky, A. J.; Patwari, P.; Sandy, J.; Plaas, A.; Ortiz, C., Individual cartilage aggrecan macromolecules and their constituent glycosaminoglycans visualized via atomic force microscopy. *J. Struct. Biol.* (2003) **143,** 242-257.
185 Attili, S.; Richter, R. P., Self-assembly and elasticity of hierarchical proteoglycan-hyaluronan brushes. *Soft Matter* (2013) **9,** 10473-10483.
186 Cho, N. J.; Kanazawa, K. K.; Glenn, J. S.; Frank, C. W., Employing two different quartz crystal microbalance models to study changes in viscoelastic behavior upon transformation of lipid vesicles to a bilayer on a gold surface. *Anal. Chem.* (2007) **79,** 7027-7035.
187 Vigerust, D. J.; Shepherd, V. L., Virus glycosylation: role in virulence and immune interactions. *Trends Microbiol.* (2007) **15,** 211-218.
188 Olofsson, S.; Hansen, J. E. S., Host cell glycosylation of viral glycoproteins - A battlefield for host defence and viral resistance. *Scand. J. Infect. Dis.* (1998) **30,** 435-440.
189 Friedman, H. M.; Cohen, G. H.; Eisenberg, R. J.; Seidel, C. A.; Cines, D. B., Glycoprotein C of herpes simplex virus 1 acts as a receptor for the C3b complement component on infected cells. *Nature* (1984) **309,** 633-635.
190 Feyzi, E.; Trybala, E.; Bergström, T.; Lindahl, U.; Spillmann, D., Structural requirement of heparan sulfate for interaction with herpes simplex virus type 1 virions and isolated glycoprotein C. *J. Biol. Chem.* (1997) **272,** 24850-24857.
191 Hua, Q.; Knudson, C. B.; Knudson, W., Internalization of hyaluronan by chondrocytes occurs via receptor-mediated endocytosis. *J. Cell Sci.* (1993) **106,** 365-375.
192 Embry, J. J.; Knudson, W., G1 Domain of Aggrecan Cointernalizes with Hyaluronan Via a CD44-Mediated Mechanism in Bovine Articular Chondrocytes. *Arthritis Rheum.* (2003) **48,** 3431-3441.
193 El Hajjaji, H.; Cole, A. A.; Manicourt, D. H., Chondrocytes, synoviocytes and dermal fibroblasts all express PH-20, a hyaluronidase active at neutral pH. *Arthritis Res. Ther.* (2005) **7,** R756-768.
194 Watarai, E.; Matsuno, R.; Konno, T.; Ishihara, K.; Takai, M., QCM-D analysis of material-cell interactions targeting a single cell during initial cell attachment. *Sens. Actuators, B* (2012) **171-172,** 1297-1302.
195 Tymchenko, N.; Nilebäck, E.; Voinova, M. V.; Gold, J.; Kasemo, B.; Svedhem, S., Reversible changes in cell morphology due to cytoskeletal rearrangements measured in real-time by QCM-D. *Biointerphases* (2012) **7,** 43.
196 Wegener, J.; Janshoff, A.; Steinem, L., The quartz crystal microbalance as a novel means to study cell-substrate interactions in situ. *Cell Biochem. Biophys.* (2001) **34,** 121-151.
197 Kunze, A.; Hesse, C.; Svedhem, S., Real-time monitoring of surface-confined platelet activation on TiO2. *Colloids Surf., B* (2014) **116,** 446-451.
198 Chen, J. Y.; Shahid, A.; Garcia, M. P.; Penn, L. S.; Xi, J., Dissipation monitoring for assessing EGF-induced changes of cell adhesion. *Biosens. Bioelectron.* (2012) **38,** 375-381.
199 Hintze, V.; Samsonov, S. A.; Anselmi, M.; Moeller, S.; Becher, J.; Schnabelrauch, M.; Scharnweber, D.; Pisabarro, M. T., Sulfated glycosaminoglycans exploit the conformational plasticity of bone morphogenetic protein-2 (BMP-2) and alter the interaction profile with its receptor. *Biomacromolecules* (2014) **15,** 3083-3092.

200 Kanzaki, S.; Takahashi, T.; Kanno, T.; Ariyoshi, W.; Shinmyouzu, K.; Tujisawa, T.; Nishihara, T., Heparin inhibits BMP-2 osteogenic bioactivity by binding to both BMP-2 and BMP receptor. *J. Cell. Physiol.* (2008) **216,** 844-850.

201 Zhou, H.; Qian, J.; Wang, J.; Yao, W.; Liu, C.; Chen, J.; Cao, X., Enhanced bioactivity of bone morphogenetic protein-2 with low dose of 2-N, 6-O-sulfated chitosan in vitro and in vivo. *Biomaterials* (2009) **30,** 1715-1724.

202 Takada, T.; Katagiri, T.; Ifuku, M.; Morimura, N.; Kobayashi, M.; Hasegawa, K.; Ogamo, A.; Kamijo, R., Sulfated Polysaccharides Enhance the Biological Activities of Bone Morphogenetic Proteins. *J. Biol. Chem.* (2003) **278,** 43229-43235.